博士論文

Studies on polyamine oxidases in *Oryza sativa* and *Selaginella lepidophylla*

（イネおよびセラギネラ・レピドフィラのポリアミン酸化酵素に関する研究）

平成 27 年度
東北大学大学院生命科学研究科
分子生命科学専攻
井上 雅貴

INDEX

Abbreviations

bp	base pair
ABA	abscisic acid
ADC	arginine decarboxylase
AIH	agmatine iminohydrolase
APT	aminopropyltransferase
BC	back conversion pathway
cDNA	complementary DNA
CPA	*N*-carbamoylputresine amidohydrolase
CuAO	copper-dependent amine oxidase
DAP	1,3-diaminopropane
DIC	differential interference contrast
dcSAM	decarboxylated *S*-adenosylmethionine
EST	Expressed sequence tag
FAD	flavin adenine dinucleotide
GA	gibberellic acid
GFP	green fluorescent protein
HPLC	high performance liquid chromatography
IAA	indole acetic acid
iP	isopentenyl adenine
JA	Jasmonic acid
JAZs	jasmonate zim-domain proteins
LC-MS/MS	liquid chromatography-tandem mass spectrometry
MS	Murashige and Skoog
MV	methyl viologen
NorSpd	norspermidine
NorSpm	norspermine
Nos-T	nopaline synthase gene terminator
ODC	ornithine decarboxylase
ORF	open-reading frame
PA	polyamine
PAO	polyamine oxidase
PCA	perchloric acid
PCR	polymerase chain reaction
Put	putrescine

qRT-PCR	real-time quantitative reverse transcription-polymerase chain reaction
RACE	rapid amplification of cDNA ends
RT	reverse transcription
SA	salicylic acid
SAM	*S*-adenosylmethionine
SAMDC	*S*-adenosylmethionine decarboxylase
SP	signal peptide
Spd	spermidine
Spm	spermine
TC	terminal catabolism pathway
TD	transmembrane domain
T-Spm	thermospermine
WT	wild type
35S	Cauliflower mosaic virus 35S promoter

Summary

Polyamines (PAs) are aliphatic compounds with low molecular masses and they are present in all living organisms. PAs play roles not only in growth, organogenesis, development and aging of plants but also in coping with various environmental stresses. In plant, major common PAs are diamine, putrescine (Put), triamine, spermidine (Spd), and tetraamines, spermine (Spm) and thermospermine (T-Spm). Some plants contain norspermidine (NorSpd) and norspermine (NorSpm) as minor uncommon PAs.

The plant PA biosynthetic pathway is well established. On the other hand, plant PA catabolic pathway(s) start to be explored. Two enzymes, copper-dependent amine oxidase and flavin adenine dinucleotide (FAD)-associated polyamine oxidase (PAO), are involved in PA catabolism. The first characterized apoplastic maize PAO and barley PAOs oxidize PAs in a terminal catabolic (TC) pathway. The recently characterized *Arabidopsis* and rice PAOs oxidize PAs in an alternative pathway, the so-called back-conversion (BC) pathway. 1,3-diaminopropane (DAP), produced by TC-type PAO, is converted to NorSpd and then NorSpm by the aminopropyl transferases with broad substrate specificity. This is a known pathway of NorSpd- and NorSpm-synthesis.

Phylogenetic analysis on angiosperm PAOs revealed that they are classified into four (I~IV) clades. Of them, the clade III members, *Arabidopsis thaliana* AtPAO5 and *Oryza sativa* OsPAO1, catabolized both Spm and T-Spm to Spd in a BC pathway.

In this study, I aim to investigate *O. sativa* and *Selaginella lepidophylla* PAOs. *O. sativa* contains 7 *PAO* genes and they are named as *OsPAO1* to *OsPAO7*. Of them, *OsPAO1*, *OsPAO3*, *OsPAO4*, *OsPAO5* and *OsPAO7* have been more or less characterized. Therefore, in chapter I, I clone the *OsPAO6* cDNA and further characterize the recombinant OsPAO6. In chapter II, I determine the enzymatic parameters of the recombinant OsPAO3, OsPAO4 and OsPAO5, and compare them with those of other OsPAOs. I examine the expressional responses of all *OsPAO*s to various phytohormones and environmental stresses, and examine the expression profiles in different tissues. Collecting the known OsPAOs' data and the data I obtain in this study, I discuss the respective roles of OsPAOs in *O. sativa*. In addition, in chapter III, I clone a clade III PAO cDNA from *S. lepidophylla* and characterize the recombinant enzyme. I discuss the similar and different features in the clade III PAOs of Selaginella and angiosperms.

I found that the provisional *OsPAO6* cDNA sequence (Accession number: NM_001069545) is incorrect and identified the correct *OsPAO6* cDNA. I further characterized the recombinant OsPAO6. This enzyme catabolized Spd, Spm and T-Spm in a TC pathway. OsPAO6 shows high identity (92%) to OsPAO7 and it is suggested to contain a signal peptide sequence. Furthermore, the GFP-fused OsPAO6 resides in the plasma membrane of plant cells. It suggests that OsPAO6 is an apoplastic enzyme.

The former laboratory members showed that (i) *OsPAO3*, *OsPAO4* and *OsPAO5* are constitutively expressed under physiological condition. The enzymes encoded by those

genes localized in peroxisomes and catabolized PAs in a BC pathway; (ii) expression of *OsPAO1* is induced by Spm and T-Spm treatment. OsPAO1 localizes in cytoplasm and functions in Spm and T-Spm catabolism in a BC reaction; (iii) *OsPAO7* is expressed in anthers and pollen. OsPAO7 catabolizes Spd and Spm in a TC reaction. I found that *OsPAO6* is responsive to drought, salinity and wounding stresses, and that it is also responsive to jasmonic acid. I also determined the kinetic parameters of OsPAO3, OsPAO4 and OsPAO5. Taken together, I discussed the role of each of the 7 OsPAOs in *O. sativa*.

The *Selaginella* plants that I examined contained NorSpd at levels of over 10 nmol/g FW and T-Spm levels of only one-tenth of NorSpd. The *Selaginella moellendorffii* genome contains a putative clade III gene, so I cloned a clade III PAO cDNA (*SelPAO5*) from *S. lepidophylla*. The recombinant SelPAO5 catalyzes the conversion of T-Spm to NorSpd. Based on these results, I propose that NorSpd is generated via T-Spm catabolism by SelPAO5. As previously mentioned, NorSpd and NorSpm are synthesized by the sequential transfer of the aminopropyl residue to DAP. The latter is formed by the action of a TC-type PAO. Therefore, the route from T-Spm to NorSpd catalyzed by PAO is a novel PA metabolic pathway.

T-Spm is an asymmetric isomer of Spm, which has a symmetrical structure. Here, I tentatively numbered the carbon atoms of T-Spm C_1 to C_{10}. AtPAO5 and OsPAO1 prefer Spm and T-Spm *in vitro* and produce Spd from both of these substrates, indicating that both enzymes oxidize the C_3-carbon. Unlike these enzymes, SelPAO5 produces NorSpd from T-Spm, indicating that SelPAO5 oxidizes the C_7-carbon of T-Spm.

It has been proposed that the T-Spm synthase gene (*ACL5*) was horizontally transferred from thermophilic bacteria or archaea to an ancestral lineage of plants. I speculate that T-Spm, produced by Selaginella ACL5, is highly cytotoxic in Selaginella and that, to reduce its toxicity, SelPAO5 catabolizes T-Spm to NorSpd, which is less toxic. During subsequent plant evolution, it is likely that the PAO in this clade acquired the ability to oxidize C_3-carbon instead of C_7-carbon to generate Spd by a BC, which occurs in the representative angiosperm AtPAO5 and OsPAO1.

Introduction

Polyamines (PAs) are aliphatic compounds with low molecular masses and they are present in all living organisms (Cohen 1998; Tabor and Tabor 1987). PAs play roles not only in growth, organogenesis, development and aging process but also in coping with various environmental stresses (Kusano et al. 2007; Eisenberg et al. 2009; Park et al. 2010).

In plant, major common PAs are diamine, putrescine (Put), and triamine, spermidine (Spd), and tetraamines, spermine (Spm) and thermospermine (T-Spm) (Fig. I-1) (Kusano et al. 2008; Takahashi and Kakehi 2010; Tibrucio et al. 2014). Some plants

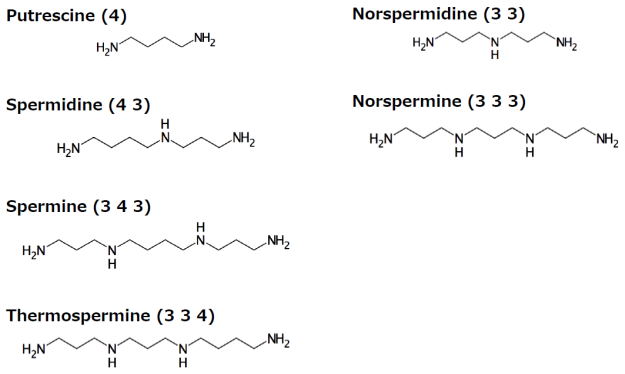

Fig. I-1. Structures of plant polyamines. Left: common polyamines; right: uncommon polyamines. The numerals in the bracket indicate the length of carbon chain between the amino residues.

contain norspermidine (NorSpd) and norspermine (NorSpm) as minor uncommon PAs (Fuell et al. 2010). PAs are derived from amino acids; ornithine, arginine and methionine. Put is synthesized from ornithine by ornithine decarboxylase (ODC) or from arginine by three sequential enzyme reactions, arginine decarboxylase (ADC), agmatine iminohydrolase (AIH) and *N*-carbamoylputresine amidohydrolase (CPA) (Fig. I-2). Spd synthesis from Put is catalyzed by Spd synthase which requires another substrate, decarboxylated S-adenosylmethionine (dcSAM). The latter is synthesized from methionine by two enzyme reactions; S-adenosylmethionine synthase (SAMS) and S-adenosylmethionine decarboxylase (SAMDC). Spm and T-Spm are derived from Spd by Spm synthase (SPMS) and T-Spm synthase (ACL5 or T-SpmS), respectively (Fig. I-2). SPDS, SPMS and ACL5 are collectively called ‘aminopropyl transferase’ because they transfer a ‘aminopropyl residue’ from dcSAM to Put or Spd. As described above, plant PA biosynthetic pathway is well established. On the other hand, plant PA catabolic pathway(s) start to be explored. Two enzymes, copper-dependent amine oxidase (CuAO: EC 1.4.3.6) and flavin adenine dinucleotide (FAD)-associated polyamine oxidase (PAO: EC 1.5.3.11), are involved in PA catabolism. The former takes homodimers of 70−90 kDa subunits, and each subunit contains a single copper ion

and a 2,4,5-trihydroxyphenylalanine quinone (TPQ) cofactor (Medda et al. 1995b; Dawkes and Phillips 2001; Kusano et al. 2015). In contrast, PAO is a monomeric enzyme. The

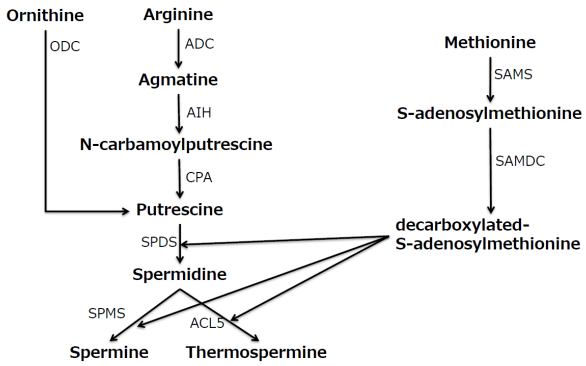

Fig. I-2. Polyamine biosynthetic pathway in plant.

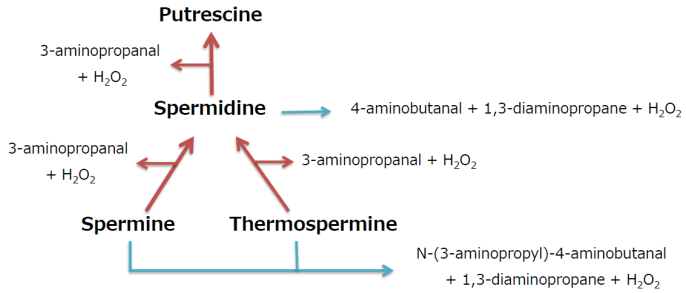

Fig. I-3. Polyamine catabolic pathways in plant. Blue arrows and red arrows indicate the terminal catabolism pathway and back conversion pathway, respectively.

first characterized apoplastic maize PAO and barley PAOs oxidize PAs in a terminal catabolic (TC) pathway. The recently characterized *Arabidopsis* and rice PAOs oxidize PAs in an alternative pathway, the back-conversion (BC) pathway (Fig. I-3) (Cona et al. 2006; Angelini et al. 2010; Wimalasekera et al. 2011a; Moschou et al. 2012). 1,3-diaminopropane (DAP), produced by TC-type PAO, is converted to NorSpd and then NorSpm by the aminopropyl transferases with broad specificity (Fig. I-4, Fuell et al. 2010).

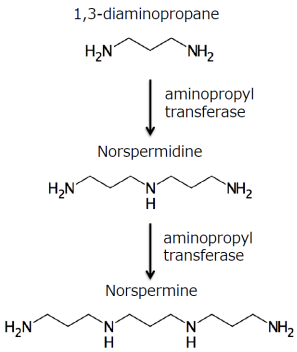

Fig. I-4. Biosynthetic pathway of NorSpd and NorSpm in plant.

The *O. sativa* genome contains 7 PAO genes. They are termed as *OsPAO1* to *OsPAO7* (Table I-1). Phylogenetic analysis on angiosperm PAOs revealed that they are at least classified into four clades, I, II, III and IV (Fig. I-5). There is no OsPAO in the clade I, three PAOs (*OsPAO2*, *OsPAO6* and *OsPAO7*) in the clade II,

Gene	Gene locus	Reference
OsPAO1	Os01g0710200	Liu et al. 2014a
OsPAO2	Os03g0193400	-
OsPAO3	Os04g0623300	Ono et al. 2012
OsPAO4	Os04g0671200	Ono et al. 2012
OsPAO5	Os04g0671300	Ono et al. 2012
OsPAO6	Os09g0368200	-
OsPAO7	Os09g0368500	Liu et al. 2014b

Table I-1. *Oryza sativa* contains 7 PAO genes. Five *OsPAO*s except *OsPAO2* and *OsPAO6* were already characterized.

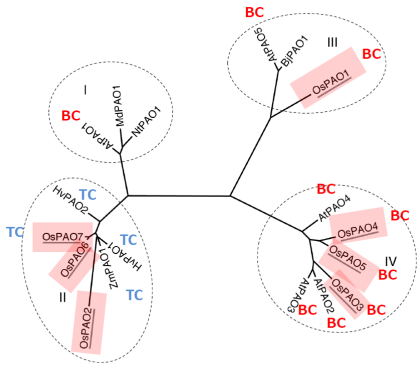

Fig. I-5. Phylogenetic tree of plant polyamine oxidases. Roman numeral indicates the clades. Seven OsPAOs are highlighted by pink color. The reaction mode of biochemically characterized PAOs is indicated as either TC or BC.

one PAO (*OsPAO1*) in the clade III, and three PAOs (*OsPAO3, OsPAO4* and *OsPAO5*) in the clade IV, respectively. So far, of them, three constitutively expressed *PAO*s, *OsPAO3*, *OsPAO4* and OsPAO5 were cloned and the respective recombinant PAO proteins were partially characterized (Table I-1, Ono et al. 2012). All of the enzymes, localized in peroxisomes, catalyzed BC-type reaction (Ono et al. 2012). Then *OsPAO1* and *OsPAO7* cDNAs were also cloned by our former laboratory member (Liu et al. 2014a, 2014b). OsPAO1 resides in cytoplasm and catalyzes BC-type reaction, whereas OsPAO7 localizes in apoplast and catalyzes TC-type reactions (Liu et al. 2014a, 2014b).

OsPAO1 and Arabidopsis AtPAO5, belonging to the clade III, function as T-Spm oxidase in host plants (Kim et al. 2014; Liu et al. 2014c) (Fig. I-5). Clade III-type PAO is present in a basal angiosperm (*Amborella trichopoda*), gymnosperms and *Selaginella moellendorffii* (vascular plants) but not in *Physcomitrella patens* and *Marchantia polymorpha* (non-vascular plants) (Kim, D.W., unpublished data).

In this Ph.D. study, I aim to investigate *Oryza sativa* and *Selaginella lepidophylla* PAOs. In chapter I, I found that the provisional *OsPAO6* cDNA sequence is incorrect and identified the correct *OsPAO6* cDNA. I further characterized the recombinant OsPAO6. In chapter II, I determined the enzymatic parameters of the recombinant

OsPAO3, OsPAO4 and OsPAO5, and examined the expressional responses of all *OsPAO*s to phytohormones, PAs and abiotic stresses. Based on all the OsPAOs' data so far obtained, I discuss a perspective view on OsPAOs in *Oryza sativa*. In addition, in chapter III, I cloned a clade III PAO cDNA (*SelPAO5*) from *S. lepidophylla* and characterized the recombinant SelPAO5. I found that SelPAO5 back-converts T-Spm to NorSpd but not to Spd. I discuss the points of agreement and difference in the clade III PAOs between Selaginella and angiosperms.

Materials and methods

Plant materials and growth conditions

The seeds of *Oryza sativa* cultivar Nipponbare were obtained from Hokuriku Agricultural Experimental Station. They were de-husked, surface-sterilized and grown hydroponically in a half-strength (1/2) Murashige-Skoog (MS) solution for 7 days, then subjected to various treatments.

Selaginella lepidophylla was purchased from Gekihana flower shop (http://shop.plaza.rakuten.co.jp/gekihana/). Other *Selaginella* varieties (Iwahiba in Japanese) were provided by a professional gardener, Mr. Kiyoshi Ishikawa.

Various treatments on rice seedlings

Rice seeds (*Oryza sativa* cv. Nipponbare) were germinated and grown on wet filter paper for 7 days at 28°C in a plant incubator and subjected to the treatment of different hormones (IAA: 20 μM; iP: 5 μM; GA: 10 μM; ABA: 100 μM; JA: 100 μM; SA: 2 mM), oxidative stresses [methyl viologen (MV): 50 μM; H_2O_2: 20 mM] and polyamines (Put, Spd, Spm and T-Spm: 500 μM each). For abiotic stresses, germinated seedlings were transferred to wet filter paper containing 200 mM NaCl (NaCl treatment), to 42°C water bath (heat), to 4°C refrigerator (cold) or on dry filter paper (dehydration) for indicated time intervals. To induce wounding stress, plants were chopped and crushed using forceps. After treatments, plant samples were harvested and RNA was extracted using RNA Sepasol-I (Nacalei-Tesque, Kyoto, Japan) according to instructions.

Chemicals

Put, Spd and Spm were purchased from Nacalai-Tesque Ltd. (Kyoto, Japan). Chemically synthesized T-Spm, NorSpm, NorSpd and N^1-acetyl Spm were kindly provided by Prof. Masaru Niitsu (Josai University) (Samejima et al. 1984; Niitsu et al. 1986). All other analytical grade chemicals were obtained from Sigma-Aldrich Corp (St. Louis, MO, USA), Wako Pure Chemical Industries Ltd. (Osaka, Japan) and Nacalai-Tesque Ltd.

Isolation of a full-length *OsPAO6* cDNA

A full-length *OsPAO6* cDNA was obtained with the combination of reverse transcription (RT)-polymerase chain reaction (PCR) and rapid amplification of cDNA ends (RACE) using the total RNA prepared from the jasmonic acid (JA)-treated rice seedlings. RACE was performed using a SMARTer RACE cDNA amplification kit (Clontech Laboratory, Inc., Takara Bio Company, Mountain View, CA, USA).

Construction of GFP fusion plasmids, particle bombardment and microscopic observation in onion cells

First the basal GFP vector was constructed. The coding region of GFP was amplified by PCR with pGFP2 (provided by Dr. N.-H. Chua) as a template and the following primer pair; forward (5'-CTTGGATCCAAGGAGATATAAGAATGGGTAAGGGAGAAGAACTTTTC-3') and reverse (5'-TATCCCGGGGCCCCCAGAGCCTCCTTTGTATAGTTCA TCCATGCCATG-3'), in which the underlined sequences were added for cloning purpose. The *Bam*HI- and *Sma*I- digested fragment was subcloned into the corresponding sites of the pBI221 vector (Invitrogen), yielding pBI221GFP. Next the internal single *Sac*I site of *SelPAO5*-coding region was mutated without changing the amino acid sequence by two step PCRs. Then second PCR on the respective mixtures of the first PCR products were performed. The coding region of *SelPAO5* was amplified by PCR using the following primer pair: SelPAO5_SmaI_F and SelPAO5_SacI_R. The resulting *SelPAO5* fragment digested with *Sma*I and *Sac*I was subcloned into the same restriction enzyme sites of pBI221GFP, yielding pBI221GFP-SelPAO5.

The full ORF region and the amino-terminal 30-amino acid region of *OsPAO6* were amplified by PCR with the primer pairs; either the combination of OSPAO6_XbaI_F and OsPAO6 full_XhoI_R1 or of OSPAO6_XbaI_F and OsPAO6_150_XhoI_R2. The *OsPAO6* fragments were digested with *Xba*I and *Xho*I. The resulting fragments were subcloned into the compatible restriction enzyme sites of the pGFP2 vector, yielding pOsPAO6 (FL)-GFP and pOsPAO6 (SP+TD)-GFP, respectively.

All the resulting GFP-PAO or PAO-GFP fusion constructs were delivered into onion bulbs by particle bombardment. After incubating the bulbs at 22°C for 16 h in darkness, the epidermal layers were peeled off and observed with a fluorescence

microscope (BX61; Olympus).

Production of recombinant OsPAOs and SelPAO5 proteins in *Escherichia coli*

OsPAO3, OsPAO4 and OsPAO5 proteins were produced in *E. coli* cells and purified as described (Ono et al. 2010). The *OsPAO6* coding region was amplified by PCR from its cDNA plasmid using the specific primer pair (Table CI-1). The fragment digested with *Bam*HI and *Sal*I was subcloned into pCold vector (Takara Co. Ltd., Kyoto, Japan) and the recombinant plasmid was transformed to *E. coli* strain Rosetta-gami B.

The *SelPAO5* coding region was amplified by RT-PCR from total RNA from *S. lepidophylla* using gene-specific primers (Table CIII-1). The amplified PCR products were digested with *Bam*HI and *Sal*I and cloned in-frame with the 6×His tag of the pCold vector (Takara Bio, Shiga, Japan), resulting in pCold-SelPAO5. After confirmation of the cloned fragments by DNA sequence analysis, pCold-SelPAO5 was transformed into *E. coli* Rosetta2 (DE3) cells, and recombinant SelPAO5 protein tagged with 6×His at the N-terminus was produced according to the manufacturer's instructions (Takara Bio, Shiga, Japan) as described (Kim et al. 2014).

PAO activity assay

Recombinant SelPAO5 oxidation activities for Spm, T-Spm, Spd, N^1-acetyl Spm and NorSpm were determined spectrophotometrically by following the formation of a pink adduct resulting from oxidation of 4-aminoantipyrine and 3,5-dichloro-2-hydroxybenzenesulfonic acid catalyzed by horseradish peroxidase as described by Kim et al. (2014). In a typical experiment, 0.5–3.0 μg of protein was added to a buffered solution containing 500 μM of each substrate, 100 μM 4-aminoantipyrine, 1 mM 3,5-dichloro-2-hydroxybenzenesulfonic acid and 10 U/mL horseradish peroxidase, and the increase in absorbance at 515 nm was measured using a multiplate reader (Tecan-M200) or spectrophotometer (Hitachi UH5300).

PA analysis by HPLC

PA analysis was performed as described (Naka et al. 2010). In brief, plant samples (0.3–0.5 g per sample) were pulverized with a mortar and pestle under liquid nitrogen. Five

volumes (2.5 mL per 0.5 g of plant sample) of 5% (v/v) cold perchloric acid were added to the resulting fine powders. The mixtures were transferred to plastic tubes and kept on ice for 1 h. After centrifugation at 15,000 × *g* for 30 min at 4°C, the supernatants were combined and filtered using a filter syringe (pore size, 0.2 μm). One milliliter of 2 N NaOH was added to 1.5 mL of plant extract, the mixture was vortexed, 10 μL of benzoyl chloride was added, the mixture was mixed and incubated at room temperature for 20 min, and then 2 mL of saturated NaCl was added. After the addition of 2 mL of diethyl ester, samples were vigorously mixed and then centrifuged at 3,000 × *g* for 10 min at 4°C for phase-separation. An aliquot (1.5 mL) of the organic solvent phase was evaporated and the residue was resuspended in 50 μL of methanol. Benzoylated PAs were analyzed with a programmable Agilent 1200 liquid chromatograph using a reverse-phase column (4.6 × 250 mm, TSK-GEL ODS-80Ts, TOSOH, Tokyo, Japan) and detected at 254 nm. For analyzing OsPAO6 reaction product(s), the benzoylated PAs were analyzed isocratically with a methanol (MeOH): water solution (see text) at a flow rate of 1 mL/ min for 20 min and detected at 254 nm (Flores and Galston 1982). For analyzing SelPAO5 reaction product(s), the acetonitrile-water system was used as a solvent system. In typical experiment, one cycle of the run consisted of a total of 60 min at a flow rate of 1 mL/min at 30°C; i.e., 42% acetonitrile for 25 min for PA separation, increased up to 100% acetonitrile during 3 min, then 100% acetonitrile for 20 min for washing, decreased down to 42% acetonitrile during 3 min, and finally 42% acetonitrile for 9 min.

LC-MS/MS analysis of the reaction product of T-Spm catalyzed by SelPAO5

The column used for LC was ACQUITY BEH C18 (2.1 × 50 mm, Waters). The sample was separated using 10–60% (linear gradient) acetonitrile containing 0.05% acetic acid. MS/MS analysis was performed at a declustering potential of 40 and a collision energy of 20 eV (Seto et al. 2014).

Dehydration treatment and tetraamine-treatment to *Selaginella* leaflets

Dehydration stress: detached *Selaginella* leaflets were placed on wet filter papers for 12 h under normal light condition, then one half of them was transferred onto dry filter papers and the residual half was transferred onto wet filter papers, and further incubated

for another 12 h. Tetraamine treatment: After 12 h incubation described above, the leaflets were separated into three groups: the first group was transferred to wet filter papers as control, and the second and third groups were transferred onto either 0.5 mM Spm or 0.5 mM T-Spm solution contained-filter papers, and further incubated another 12 h.

Quantitative reverse transcription-polymerase chain reaction (qRT-PCR) assay

qRT-PCR analysis was performed by StepOne Real-Time PCR System (Applied Biosystems) using SYBR ®Green RT-PCR Kit (FastStart Universal SYBR Green Master, ROX). A standard curve was constructed from different genes and the values were normalized to *Actin* levels. The primers used for qRT-PCR were described in Table CII-2 and Table CIII-1.

Statistical analysis

Student's *t* tests were used for statistical analysis and were performed using Microsoft Excel statistical tools.

Table CI-1. The primers used for cloning *OsPAO6* cDNA and constructing the expression plasmid vector.

Experiment	Name	Sequence(5' -3')
RT-PCR	OsPAO6_F1	GGATCCATGGAAGAAAACAAGGTCTCCATG
	OsPAO6_F2	GCTTCCGCTCCGACTTTGACAGCCTTGCCCA
	OsPAO6_F3	CCAAGGCAGAGATCATGGAGGTT
	OsPAO6_R1	GTCGACCCTCGATCAACAAATTGTGGAA
	OsPAO6_R2	CCTCGATGAACAAATTGTGGAA
	OsPAO6_R3	CTGGGCAAGGCTGTCAAAG
	OsPAO6_R4	AGAGGCCTCCGTCCTTGTAGT
RACE-PCR	UPM_F	CTAATACGACTCACTATAGGGCAAGCAGTGGTATCAACGCAGAGT
	UPMs_F	CTAATACGACTCACTATAGGGC
	OsPAO6_GSP_R	GATTACGCCAAGCTTTGAGCTTCAGGCGGGCGTCGGCG
	OsPAO6_NGSP_R	GATTACGCCAAGCTTCGAAGTAGGTGTCGTCTCCG
Plasmid	OsPAO6_BamHI_F	GGATCCATGACGAAGCCCACGACGAT
construction	OsPAO6_SalI_R	GTCGACCTAGCCGTGCTTGCCCCC

Table CI-2. The primers used for generating the GFP fusion plasmids.

Experiment	Name	Sequence(5' -3')
GFP::OsPAO6	OsPAO6_XbaI_F	TGC TCTAGAATGACGAAGCCCACGACGATG
Plasmid	OsPAO6 full_XhoI_R1	TGC CTCGAG GCCGTGCTTGCCCCCGAC
construction	OsPAO6_150_XhoI_R2	TGC CTCGAG CCATATCCGCTTCCCCGCTGAG

Table CII-2. The primers used for qRT-PCR analysis of *OsPAO*s.

Experiment	Name	Sequence(5' -3')
qRT-PCR	OsPAO1_F	CAAGCTGTTCATGGAGGTGG
	OsPAO1_R	TTGGACACGTGTCCCCGGAA
	OsPAO2_F	ACGAATTCGACATGGCTGTGT
	OsPAO2_R	GGTGCTCGCGTAGAGGAAGA
	OsPAO3_F	TTTCTATTGCGAAGGCCATTG
	OsPAO3_R	ATGCGGCACAAATACCACTGA
	OsPAO4_F	TGCCCGCCAATTCAATGGAGTGAC
	OsPAO4_R	ACTTGATTATGTTTGCCTTGA
	OsPAO5_F	CATCCAGAGGTACAACAAAACTAT
	OsPAO5_R	TTCAAACTTGATGATATTTGCTTTAA
	OsPAO6_F	AGGCGCAAGCATTTTCATG
	OsPAO6_R	CCTCGATGAACAAATTGTGGAA
	OsPAO7_F	CTTGCAGGTATCTATGCCTAATTTGT
	OsPAO7_R	AAATGGTTTACATCTCCGGTCTCT
	OsEF-1α_F	TTTCACTCTTGGTGTGAAGCAGAT
	OsEF-1α_F	GACTTCCTTCACGATTTCATCGTAA

Table CIII-1. The primers used in chapter III.

Experiment	Name	Sequence(5' -3')
Inverse PCR	SelPAO5_F1	ATCCGAGTCTTCGAGCTTTG
	SelPAO5_F2	AAGGTCGAGGTCATGCAGAG
	SelPAO5_R1	GCTTGCCACCAAATACCATC
	SelPAO5_R2	GACGGTCGAGATGGAGAATG
	SmPAO_6_7_F	GATCGGTGCTACGTGGATTC
	SmPAO_6_7_R	CAGCTTGTCCACGACACCGAAG
Plasmid construction	SelPAO5_BamHI_F	GCGGATCCATGGAGCTGAAAATATGCCAATCTC
	SelPAO5_SalI_R	GCGTCGACTTACGATTCCAGGATTTTGTAGTGC
	SelPAO5_SmaI_F	AGCCCGGGATGGAGCTGAAAATATGCCAA
	SelPAO5_SacI_R	GGGAGCTCTTTACGATTCCAGGATTTTGTA
	SelPAO5 Sac_Mut_F	GGCCTCTATAAGGAACTCGTTGCCGAG
	SelPAO5 Sac_Mut_R	GATCTCGGCAACGAGTTCCTTATAGAG
qRT-PCR	SelPAO5_F	GATGGAGCCCACGGAAGA
	SelPAO5_R	CGGGCCGGTGAATAAGC
	SmACT_F	AGCGGAGGCAGCACAATG
	SmACT_R	GCCGTGATTTCCTTGCTCAT

Chapter I

Identification and characterization of *Oryza sativa* polyamine oxidase 6 (*OsPAO6*) gene

Introduction

As I mentioned, *O. sativa* contains 7 PAO genes. Of them, *OsPAO1*, *OsPAO3*, *OsPAO4*, *OsPAO5* and *OsPAO7* cDNAs were already cloned and characterized (Ono et al. 2012; Liu et al. 2014a, 2014b, 2014c). Ono et al. (2012) showed that the uncharacterized two PAO genes, *OsPAO2* and *OsPAO6*, are expressed at quite scarce levels under physiological condition (Fig. CI-1) which is supported by rice array data (RiceXPro: http://ricexpro.dna.affrc.go.jp/). Actually the former laboratory members tried to clone them, but failed.

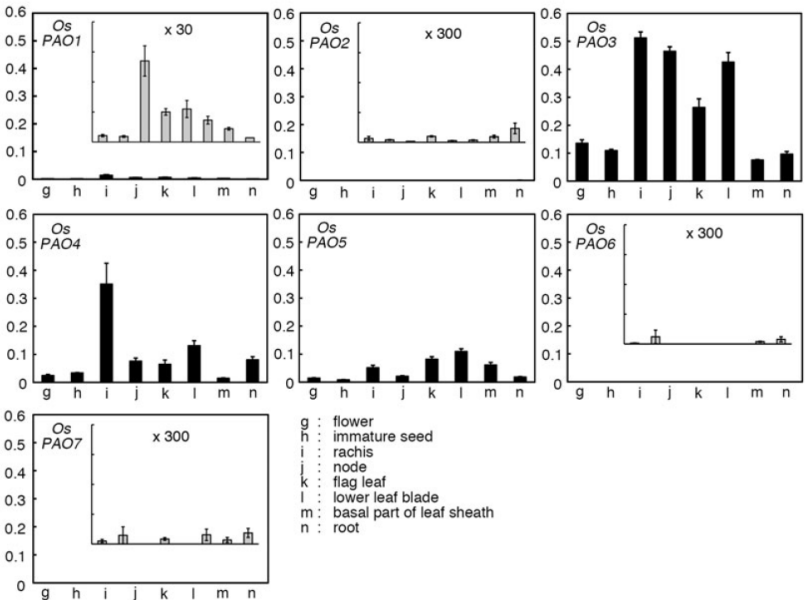

Fig. CI-1. Expressional profiles of 7 PAO genes of *O. sativa* at flowering stage. This figure was cited from the article of Ono et al. (2012).

In this chapter, I describe the cloning of the *OsPAO6* full-length cDNA and characterize the recombinant OsPAO6 enzyme.

Results

Isolation of *OsPAO6* cDNA

According to the public database (National Center for Biotechnology Information), the coding region of *OsPAO6* cDNA comprises 1,623 base pairs (bp) (Accession number NM_001069545). Eight EST (Expressed sequence tag) clones of *OsPAO6* were reported (http://www.ncbi.nlm.nih.gov/UniGene/clust.cgi?ORG=Os&CID=73758) (Fig. CI-2A). Counting the information, I designed 7 *OsPAO6*-specific primers. Using the F_3 and R_2 primer pair (see Fig. CI-2A), I examined the *OsPAO6* expression and found that the gene is responsive to jasmonic acid (JA) (Fig. CI-2B). I further performed the reverse transcription-polymerase chain reaction (RT-PCR) with several primer combinations on the same cDNA derived from JA treated seedlings as a template. With F_2 and R_2 primer combination, a single DNA fragment of approximately 1,200 bp in size was detected (Fig. CI-2C). DNA sequencing revealed that the fragment corresponds to the nucleotide positions (np) 450 to 1,623 of the provisional 1,623 bp-open reading frame (ORF). However, when I used the forward primer F_1 in combinations with all the reverse primers I tested no PCR products could be detected (Fig. CI-2C), suggesting that the 5' region of the full-length cDNA is different from the reported cDNA sequence. Therefore, I performed the 5'-rapid amplification of cDNA ends (RACE) experiment. As shown in Fig. CI-3A, I used the two primer pairs; the one is Universal primer mix (UPM) and the gene specific primer 1 (GSP1), the other is Universal primer short (UPS) and the nested gene specific primer 1 (NGSP1). With UPM and GSP1 primer pair, no distinct fragment was observed (Fig. CI-3B, lane 2). The second PCR using the UPS and NGSP1 on the aliquot of the PCR product with UPM and GSP1 gave an approximately 0.8 kb-fragment (Fig. CI-3B, lane 1). The resulting full-length *OsPAO6* cDNA is 1,742 bp (Accession number, LC107620). The coding sequence of it starts at the np 39 and ends at the np 1,529, which encodes a 497-amino acid protein (Fig. CI-4). In Fig. CI-5, the open-reading frame region of the new *OsPAO6* cDNA was compared with that of the old *OsPAO6*. Next the new OsPAO6 amino acid sequence and the old one (540-amino acid protein) were aligned (Fig. CI-6). As expected, the amino-terminal regions were quite different. Of interest, the newly assigned OsPAO6 showed high identity (92%) to OsPAO7 (Fig. CI-7). To confirm the *OsPAO6* cDNA sequence result, I checked the *O. sativa* chromosome 9 genome sequence. As shown in Fig. CI-8, the 5'-distal region of *OsPAO6* cDNA was totally matched with the sequence of np 12,759,144 and np 12,758,973 (minus strand) of the chromosome 9. The previous *OsPAO6* cDNA sequence is derived from twelve exons (E_1 to E_{12}), whereas the

OsPAO6 cDNA sequence isolated in this study is derived from nine

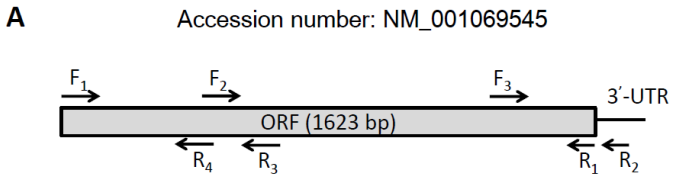

C

Primer combination	Results
F1 + R1	No PCR product
F1 + R2	No PCR product
F2 + R2	One PCR product (1,200 bp)
F1 + R3	No PCR product
F1 + R4	No PCR product

Fig. CI-2. Cloning of *OsPAO6* cDNA. A. Schematic illustration of *OsPAO6* cDNA available in the public database and the position and orientation of the primers. B. RT-PCR result using F_3 and R_2 primers which showed that *OsPAO6* was responsive to JA. C. RT-PCR results using the other primer combination.

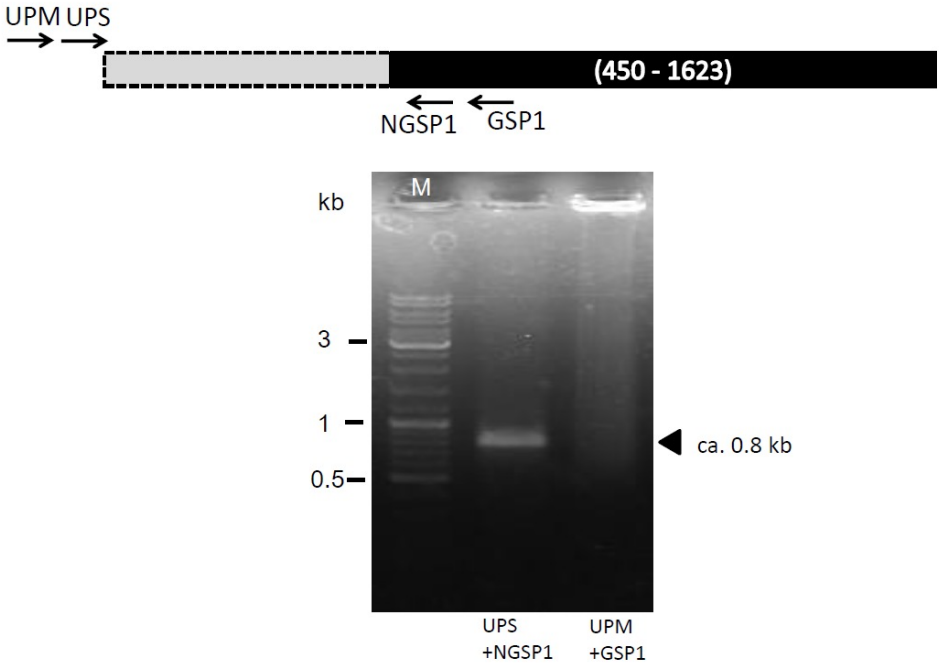

Fig. CI-3. 5'-RACE experiment for isolating the 5'-distal region of *OsPAO6* cDNA. Upper figure: the black box region was already cloned and it was totally matched the reported *OsPAO6* cDNA sequence, while the grey box region was still missing. The position and orientation of the primers were also shown. Lower figure: left lane, DNA size marker; middle lane, PCR result using UPS and NGSP1 primers and the aliquot (as DNA template) of the PCR product (right lane) using UPM and GSP1 primer pair on the

cDNA prepared from JA-treated *O. sativa* seedlings. Black arrowhead indicated that the size of fragment was approximately 0.8 kb.

```
   1  GTGCCAAGAAGGGAGATCGAGAGTACTTGAAAGACAGTATGACGAAGCCCACGACGATGG  61
                                          M  T  K  P  T  T  M

  61  CCATTTTTCTTGTCTTAGCGCTATCCATAGCACAGCTTCTTCCGTCCCTCGTCGCTGGCA  121
      A  I  F  L  V  L  A  L  S  I  A  Q  L  L  P  S  L  V  A  G

 121  CCGGCCGGCCAAGGGTCATCATTGTTGGCGCTGGCATATCCGGTATCTCAGCGGGGAAGC  181
      T  G  R  P  R  V  I  I  V  G  A  G  I  S  G  I  S  A  G  K

 181  GGATATGGGAGGCTGGGATAGCAGACGTATTGATCTTAGAGGCGACAGACCGCATTGGCG  241
      R  I  W  E  A  G  I  A  D  V  L  I  L  E  A  T  D  R  I  G

 241  GGCGGATGCACAAGCAGAGTTTCGCCGGCGTCAATGTGGAGATCGGTGCCAACTGGGTGG  301
      G  R  M  H  K  Q  S  F  A  G  V  N  V  E  I  G  A  N  W  V

 301  AGGGCGTCAATGGCGAAAAGAAGAACCCCATTTGGCCCATCGTCAACTCCACCCTCAAGC  361
      E  G  V  N  G  E  K  K  N  P  I  W  P  I  V  N  S  T  L  K

 361  TCAGAAGCTTCCGCTCCGACTTTGACAGCCTTGCCCAGAACGTCTACAAGGACGGAGGCC  421
      L  R  S  F  R  S  D  F  D  S  L  A  Q  N  V  Y  K  D  G  G

 421  TCTGTGACGAAGCATACGTGCAGAAGAGAATGGATCGGGCAGATGAAGTGGACAAGAGTG  481
      L  C  D  E  A  Y  V  Q  K  R  M  D  R  A  D  E  V  D  K  S

 481  GGGAGAATCTCTCCGCCACACTGCACCCAAGCGGCCGGGACGACATGTCAATCCTTTCAA  541
      G  E  N  L  S  A  T  L  H  P  S  G  R  D  D  M  S  I  L  S

 541  TGCAACGGCTCAACGATCACCTACCCAACGGCCCGTCGTCGCCGGTGGACATGGCGGTGG  601
      M  Q  R  L  N  D  H  L  P  N  G  P  S  S  P  V  D  M  A  V

 601  ACTACTTCACCTACGACTACGAGTTCGCCGAGCCGCCGCGCGTGACCAGCCTGCAGAACA  661
      D  Y  F  T  Y  D  Y  E  F  A  E  P  P  R  V  T  S  L  Q  N

 661  CCGTTCCCCTCCCCACCTTCACCGACTTCGGAGACGACACCTACTTCGTCGCCGACCAAC  721
      T  V  P  L  P  T  F  T  D  F  G  D  D  T  Y  F  V  A  D  Q

 721  GTGGCTACGAGTCCGTCGTCCACCACCTCGCCGGCCAGTACCTCAACGCCGACAAGTCCG  781
      R  G  Y  E  S  V  V  H  H  L  A  G  Q  Y  L  N  A  D  K  S

 781  GCAACATCGCCGACGCCCGCCTGAAGCTCAACAAGGTGGTGCGTGAGATCTCCTACTCCT  841
      G  N  I  A  D  A  R  L  K  L  N  K  V  V  R  E  I  S  Y  S

 841  CGACCGGCGTCACCGTGAAGACGGAGGACAACTCGACGTACCAGGCAGACTATGTCATGG  901
      S  T  G  V  T  V  K  T  E  D  N  S  T  Y  Q  A  D  Y  V  M

 901  TTTCTGCGAGCTTGGGAGTCCTGCAGAGCGATCTCATACAGTTCAAGCCACAGCTGCCTT  961
      V  S  A  S  L  G  V  L  Q  S  D  L  I  Q  F  K  P  Q  L  P

 961  CTTGGAAGATTCTTGCGATCTACCAATTCGACATGGCCGTGTACACCAAGATATTCGTCA 1021
      S  W  K  I  L  A  I  Y  Q  F  D  M  A  V  Y  T  K  I  F  V

1021  AGTTCCCCAAGAAATTCTGGCCCGAAGGGGCAGGGAGGGAGTTCTTCCTCTACGCGAGCA 1081
      K  F  P  K  K  F  W  P  E  G  A  G  R  E  F  F  L  Y  A  S

1081  CCAGGAGAGGCTACTACGGAGTCTGGCAGGAGTTTGAGAAGCAATACCCGGATGCCAATG 1141
      T  R  R  G  Y  Y  G  V  W  Q  E  F  E  K  Q  Y  P  D  A  N

1141  TGCTCCTGGTGACGGTGACCGACGAGGAGTCGAGGCGGATCGAGCAGCAGCCGGACAGCC 1201
      V  L  L  V  T  V  T  D  E  E  S  R  R  I  E  Q  Q  P  D  S

1201  AGACCAAGGCAGAGATCATGGAGGTTGTGAGGTGCATGTTCCCTGACGAGGATGTCCCCG 1261
      Q  T  K  A  E  I  M  E  V  V  R  C  M  F  P  D  E  D  V  P

1261  ACGCCACCGACATCCTCGTCCCGAGATGGTGGTCCGACAGGTTCTTCCGGGGCAGCTTCT 1321
      D  A  T  D  I  L  V  P  R  W  W  S  D  R  F  F  R  G  S  F

1321  CCAACTGGCCCATCGGCGTCAGTCGCTACGAGTATGACCAGCTCAGGGCGCCGGTTGGGA 1381
      S  N  W  P  I  G  V  S  R  Y  E  Y  D  Q  L  R  A  P  V  G

1381  GAGTGTACTTCACCGGTGAGCACACGAGCGAGCGCTACAATGGCTATGTCCATGGAGCTT 1441
      R  V  Y  F  T  G  E  H  T  S  E  R  Y  N  G  Y  V  H  G  A

1441  ATCTTGCAGGTATTGACTCTGCAGAGATTCTGATCAACTGTGCACAGAAGAAGATGTGCA 1501
      Y  L  A  G  I  D  S  A  E  I  L  I  N  C  A  Q  K  K  M  C

1501  AATATAATGTCGGGGGCAAGCACGGCTAGTTTGTGGAGGCGCAAGCATTTTCATGATGGG 1561
      K  Y  N  V  G  G  K  H  G  *

1561  ATGAGAAATGTGAGATTCCACAATTTGTTCATCGAGGTGTAAAGCAATTTGAGGAAAAAG 1621

1621  TGTTTACACTAATTGTTTACTTATGCTATTTCTTGTTGCTGAATATATATTTCAGCAGTT 1681

1681  CAGCTGATGTATATATGTGCTATTGTTTCGAAATGAATAAAATCTTGCGTAGATTTGTAA 1741

1741  AA
```

Fig. CI-4. The newly assigned *OsPAO6* cDNA sequence (accession number, LC107620) and the deduced OsPAO6 amino acid sequence. Asterisk indicates the stop codon.

Fig. CI-5. Comparison of the nucleotide sequences of new and old *O. sativa* polyamine oxidase 6 ORFs.

Fig. CI-6. Comparison of new and old OsPAO6 amino acid sequences. Identical amino acid was indicated by asterisk.

Fig. CI-7. Comparison of new OsPAO6 and OsPAO7 amino acid sequences. Identical amino acid was indicated by asterisk.

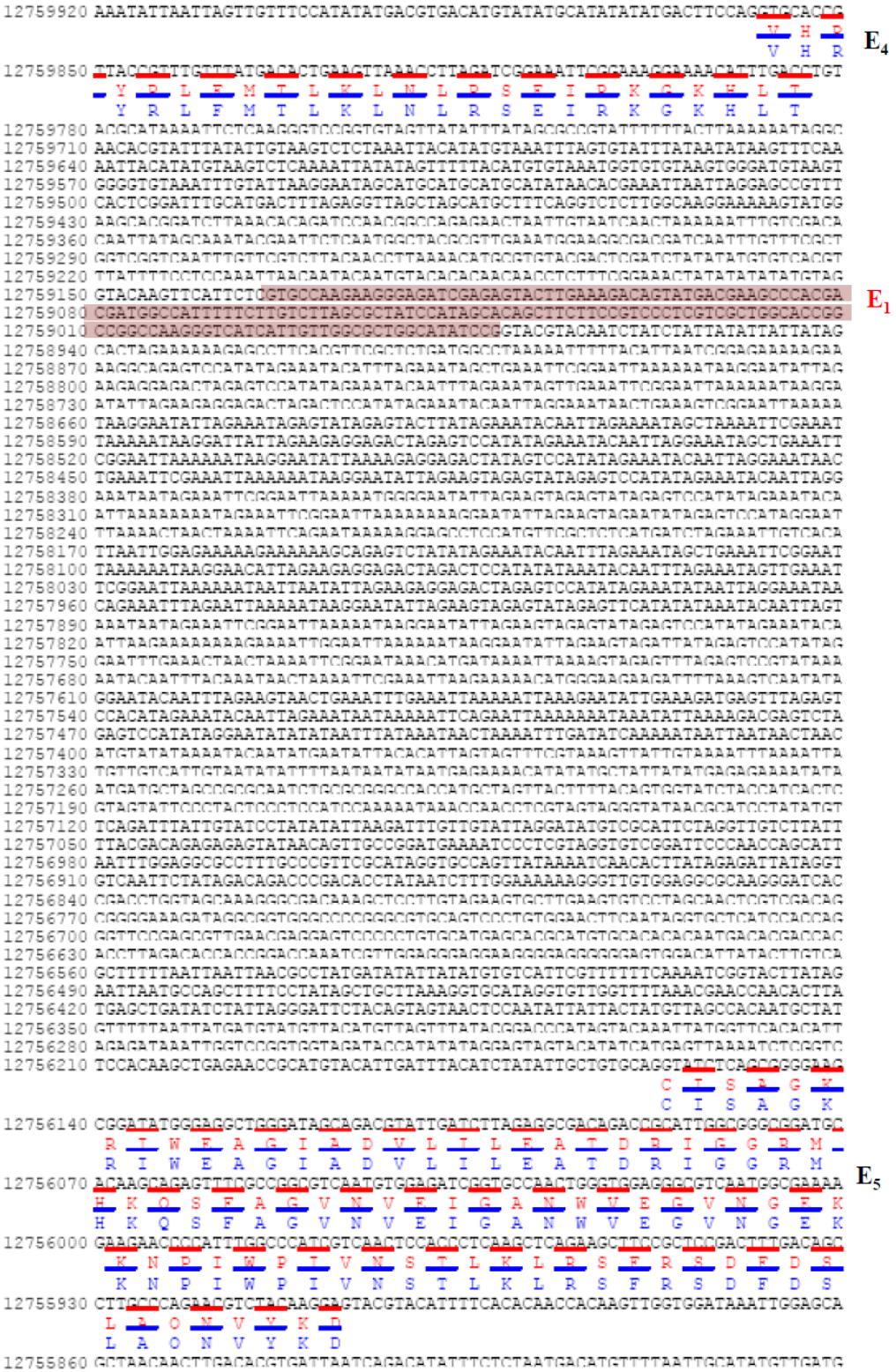

Fig. CI-8. Assignment of the 5'-distal region of *OsPAO6* transcript on the genome DNA sequence of *O. sativa* chromosome 9. The provisional E_4 and E_5 were indicated by black letters, while the newly assigned E_1 and E_2 were indicated by red letters. The E_1 region was highlighted by transparent pink color. The new intron follows the GT-AG rule.

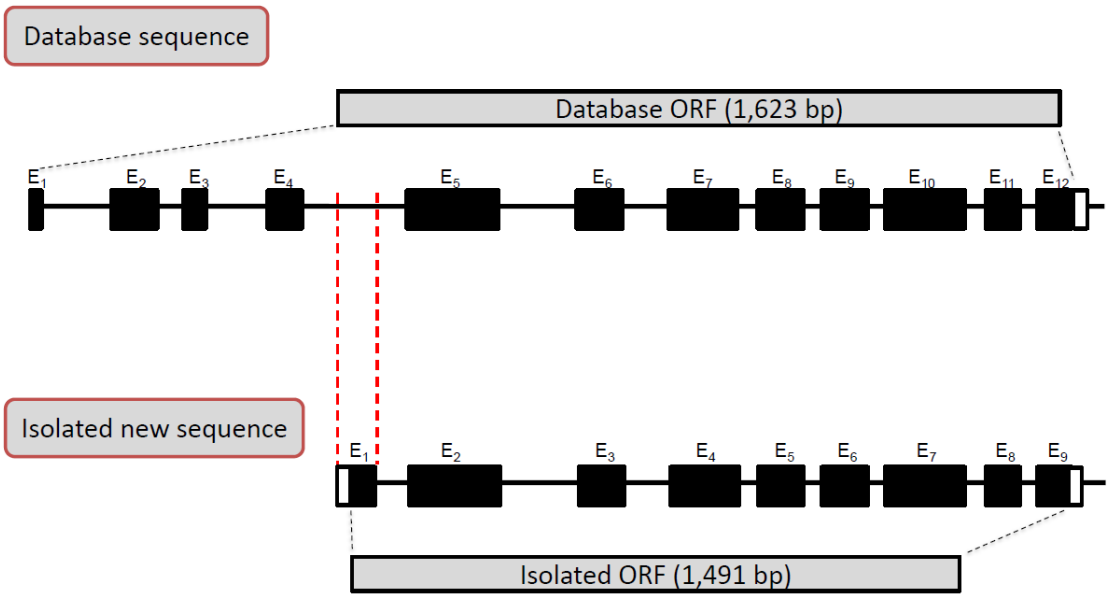

Fig. CI-9. The genome assignment of the new *OsPAO6* transcript. The upper figure is derived from the NCBI information. The provisional assignment indicates that *OsPAO6* is consisting of 12 exons and 11 introns, whereas the newly isolated *OsPAO6* is consisting of 9 exons and 8 introns. The E_2~E_9 totally corresponds to the old E_5~E_{12}, respectively. White box and black box indicate the untranslated region and the coding region, respectively. The newly identified E_1 corresponds to the region between the previous E_4 and E_5 which is highlighted by the red botted lines. See also Fig. CI-8.

exons. The difference in the genome assignment between the former *OsPAO6* and new *OsPAO6* cDNA sequences was illustrated in Fig. CI-9.

Subcellular localization of OsPAO6 in plant cells

SignalP ver 4.1 program (http://www.cbs.dtu.dk/services/SignalP/) predicts that a signal peptidase recognizes between 27 and 28 amino acid positions of OsPAO6 (Fig. CI-10). To test the subcellular localization of OsPAO6 in plant cells, I generated the two green fluorescent protein (GFP)-fusion constructs. The one is the full-length ORF region of OsPAO6-fused to the GFP gene, which termed FL. The other is the signal peptide (SP)-transmembrane domain (TD) region of OsPAO6-fused to GFP gene, which termed SP+TD. Those constructs were delivered to onion epidermal cells by particle bombardment (PDS-1000/He, Bio-Rad). The result indicated that both the FL fusion and the SP+TD fusion localized in plasma membrane matching to the positive plasma membrane-localized marker, OsPIP2;1 (plasma membrane intrinsic protein) (Fig. CI-11). Therefore, it is likely that OsPAO6 targets the apoplastic space via its signal peptide.

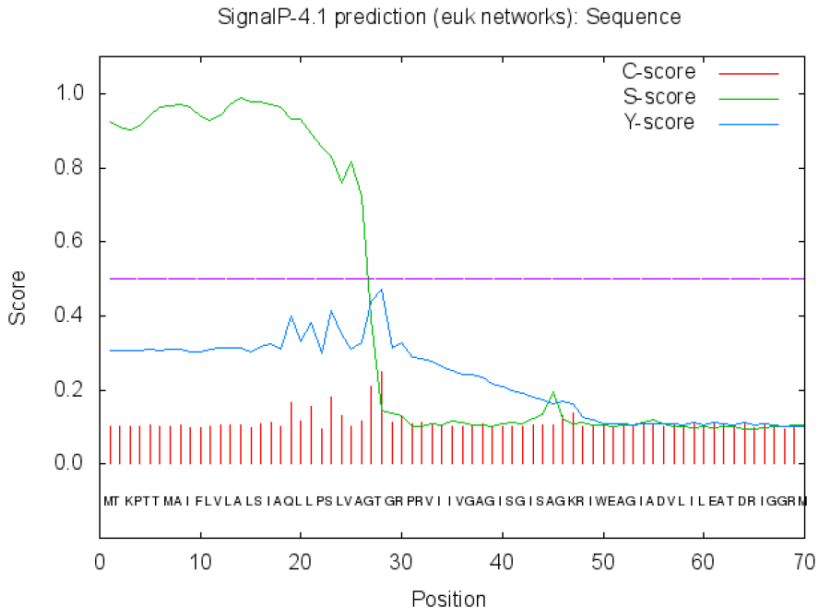

Fig. CI-10. Signal-P program predicts that the amino acid portion from 1 to 27 of OsPAO6 amino acid sequence is a signal peptide.

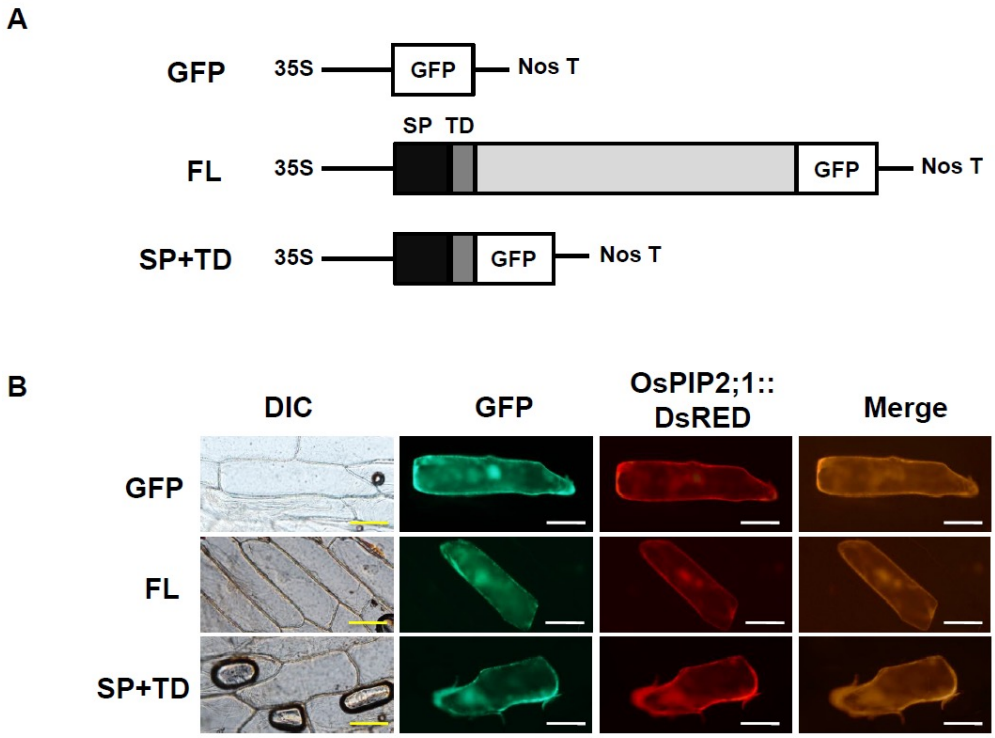

Fig. CI-11. Subcellular localization of OsPAO6 in plant cells. A. Schematic drawing of the OsPAO6::GFP fusion constructs. *OsPIP2;1* encodes a plasma membrane intrinsic protein (a form of aquaporin), is a plasma membrane-localized marker. FL: the full-length region of OsPAO6 was fused to the GFP; SP+SD: the signal peptide region of OsPAO6 was fused to the GFP. 35S, Cauliflower mosaic virus 35S promoter; Nos T, the terminator region derived from the nopaline synthase gene. B. Subcellular localization of OsPAO6 in onion epidermal cells. Bar corresponds to 10 μm.

Production of the recombinant OsPAO6 in *E. coli*

I am going to express and purify the OsPAO6 protein using the *E. coli*-pCold vector system. However, at this moment, I cannot purify it homogenously.

Chapter summary

In this chapter, I successfully isolated *OsPAO6* cDNA. The critical points are that (1) I found the expression condition of *OsPAO6*; (2) the 5'-distal region of the newly identified *OsPAO6* cDNA sequence was different from the one of the old *OsPAO6* cDNA sequence. While the old *OsPAO6* cDNA sequence was derived from 12 exons and 11 introns of the chromosome 9, the newly identified *OsPAO6* cDNA sequence was derived from 9 exons and 8 introns. Furthermore, the 1st exon was found inside the sequence of the previous 4^{th} intron. The deduced OsPAO6 amino acid sequence is a 497-long. It showed the more than 92% identity to OsPAO7. OsPAO6 protein localizes in plasma membrane of plant cells. Counting the information that the amino-terminal region of OsPAO6 may function as a signal peptide, predicted by SignalP program, it suggests that OsPAO6 is a secondly identified apoplastic PAO enzyme in *O. sativa*.

To reveal the reaction mode of OsPAO6, I tried to produce and purify the recombinant OsPAO6. Unfortunately I cannot succeed it.

Chapter II

A perspective view on polyamine oxidases in *Oryza sativa*

Introduction

In chapter I, I identified *OsPAO6* cDNA and characterized the recombinant OsPAO6. My further work on it showed that OsPAO6 acts as TC-type PAO. So now, all OsPAOs except OsPAO2 were characterized. In cases of OsPAO3, OsPAO4 and OsPAO5, it is known that they localize in peroxisomes and act as BC-type enzymes (Ono et al. 2012). They further showed that OsPAO3 prefers Spd over the other PAs, while both OsPAO4 and OsPAO5 prefer Spm as substrate (Fig. CII-1). However, their enzymatic parameters are not analyzed yet. From the expression analysis, I have learned that *OsPAO3*, *OsPAO4* and *OsPAO5* are constitutively expressed both at the seedling stage and at the flowering stage, and that the other four members, *OsPAO1*, *OsPAO2*, *OsPAO6* and *OsPAO7*, are expressed at a scarce level under the non-stressed condition (Ono et al. 2012). Liu et al. (2014a, 2014b) reported that *OsPAO1* is induced by tetraamines and that *OsPAO7* is expressed in anthers and pollens. In addition, I showed that *OsPAO6* is responsive to JA (Chapter I).

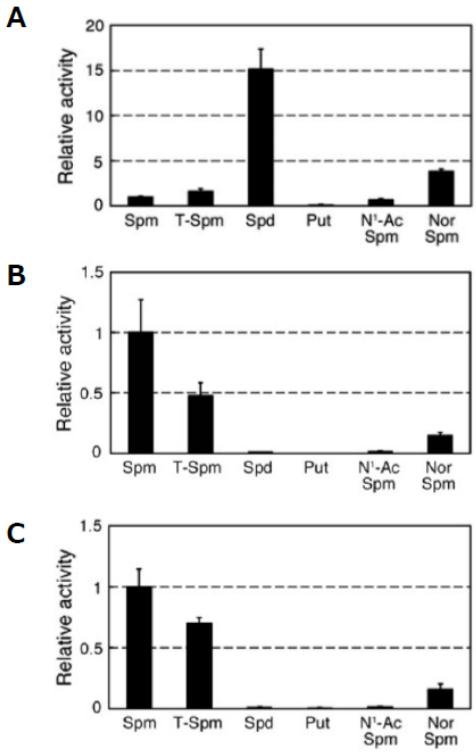

Fig. CII-1. PA substrate specificity of OsPAO3 (A), OsPAO4 (B) and OsPAO5 (C). Those figures were cited from the article of Ono et al. (2012).

In this chapter, I determine the kinetic parameters of OsPAO3, OsPAO4 and OsPAO5. Furthermore, to find a clue(s) to discuss the division of roles of 7 *OsPAO*s, I

test the effect of phytohormones, reactive oxygen species, abiotic stresses and PAs on 7 *OsPAO*s' expression. I further examine whether *OsPAO6* is also expressed in flower. Taken all the OsPAOs' information, I discuss the roles of the respective PAOs in *O. sativa*.

Results

Kinetics analysis of the recombinant OsPAO3, OsPAO4 and OsPAO5

I just followed the protocol described by Ono et al. (2012) and purified the recombinant OsPAO3, OsPAO4 and OsPAO5 in the *E. coli* system. Using the purified enzymes, I determined the kinetic parameters. Using Lineweaver-Burk plot, I obtained K_m and V_{max} values. k_{cat} value is calculated as follows:

$$k_{cat} = \frac{V_{max}}{[E]_T} \ (s^{-1})$$

Table CII-1. Kinetic parameters of the recombinant OsPAO3 (A), OsPAO4 (B) and OsPAO5 (C).

A

	Spd(pH 8.5)	Spm(pH 8.5)	T-Spm(pH 8.5)
kcat (s^{-1})	0.4427±0.138	0.0331±0.021	0.0775±0.059
Km (μM)	156.4±37.7	172.2±45.7	549.9±46.6
kcat/Km ($M^{-1}s^{-1}$)	2897±867	186.0±91.5	136.7±99.1

B

	Spd(pH 7,0)	Spm(pH 7.0)	T-Spm(pH 7.0)
kcat (s^{-1})	3.173±0.747($x10^{-3}$)	0.2789±0.0875	0.3971±0.186
Km (μM)	12.40±3.11	105.1±25.2	409.4±173
kcat/Km ($M^{-1}s^{-1}$)	257.8±15.8	2600±349	933.4±93.6

C

	Spd(pH 7.5)	Spm(pH 7.5)	T-Spm(pH 7.5)
kcat (s^{-1})	2.208±0.844($x10^{-3}$)	0.6291±0.305	1.088±0.764
Km (μM)	77.05±24.7	133.4±25.4	534.9±369
kcat/Km ($M^{-1}s^{-1}$)	28.10±4.71	4430±1764	1852±645

First, the kinetic parameters of OsPAO3 were calculated. OsPAO3 preferred Spd over Spm and T-Spm. In fact, at optimum pH 8.5, the k_{cat}/K_m (catalytic efficiency) for Spd was 2,897 $\pm$ 867 M^{-1} s^{-1}, while those for Spm and T-Spm were 186 $\pm$ 92 M^{-1} s^{-1} and 136 $\pm$ 99 M^{-1} s^{-1}, respectively (Table CII-1A). Then the kinetic parameters of OsPAO4 and OsPAO5 were determined. Both the enzymes preferred Spm. The k_{cat}/K_m for Spm of OsPAO4 and OsPAO5 were 2,600 $\pm$ 349 M^{-1} s^{-1} and 4,430 $\pm$ 1,764 M^{-1} s^{-1}, respectively,

while those for T-Spm of OsPAO4 and OsPAO5 were 933 ± 94 M^{-1} s^{-1} and 1,852 ± 645 M^{-1} s^{-1} (Table CII-1B,C). Both the enzymes did not prefer Spd as substrate, especially OsPAO5. Those for Spd of OsPAO4 and OsPAO5 were 258 ± 16 M^{-1} s^{-1} and 28 ± 4.7 M^{-1} s^{-1} (Table CII-1B,C).

Expressional change of *OsPAO*s to phytohormones

To understand the respective roles of *OsPAO*s, I first applied various phytohormones to 7-day-old rice seedlings and examined the transcript levels by qRT-PCR analysis. The primers used for these qRT-PCR experiments were listed in Table CII-2. *OsPAO5* was induced to ~4.5-fold levels compared to those of non-stress condition at 6 h by indole acetic acid (IAA) treatment, whereas *OsPAO2* and *OsPAO6* were negatively regulated by IAA (Fig. CII-2). Isopentenyl adenine (iP, active cytokinin) induced *OsPAO1* and *OsPAO7* ~5-fold and ~20-fold, respectively, at 12 h, whereas *OsPAO2* and *OsPAO6* were down-regulated (Fig. CII-2). Gibberellic acid (GA) and abscisic acid (ABA) did not have much effect on *OsPAO* expression. *OsPAO5* and *OsPAO7* were transiently induced to ~3-fold levels by GA, whereas *OsPAO1* transcripts reached to ~2-fold levels at 6 h (Fig. CII-2). The transcript levels of *OsPAO2* and *OsPAO6* were again down-regulated by GA and ABA (Fig. CII-2). Salicylic acid (SA) suppressed the

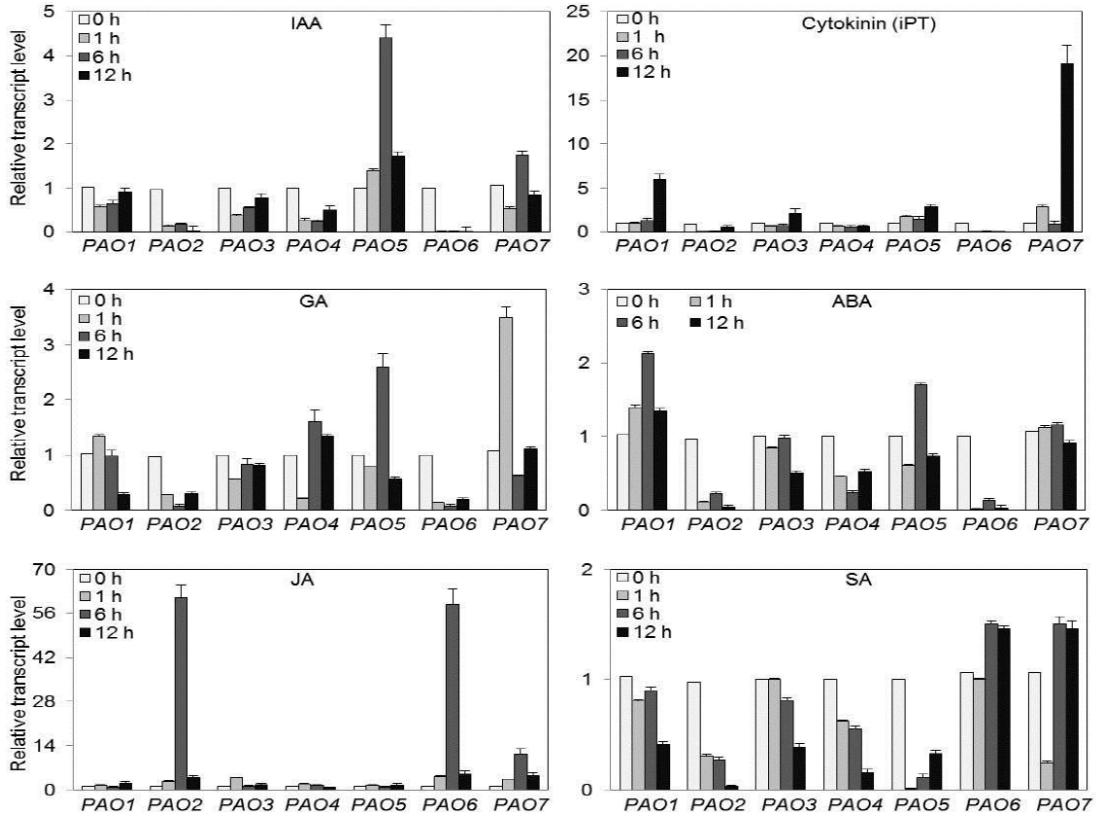

Fig. CII-2. Effect of phytohormones on the expression of *OsPAO*s.

expression of *OsPAO2*, *OsPAO4* and *OsPAO5*. On the other hand, *OsPAO6* and *OsPAO7* were slightly (~1.5-fold) induced at 6 h and 12 h (Fig. CII-2). Most striking effect was observed in JA treatment. At 6 h after JA treatment, *OsPAO2* and *OsPAO6* transcripts reached to around 60-fold levels (Fig. CII-2).

Expressional change of *OsPAO*s to abiotic stresses

Next I examined the effects of abiotic stresses on the expression of *OsPAO*s. Upon heat (42°C) *OsPAO3*, *OsPAO4* and *OsPAO6* were rapidly and transiently induced at 10~30 fold levels, while the residual members were not responsive (Fig. CII-3). Cold induced the expression of *OsPAO4, OsPAO6* and *OsPAO7* about 3 to 4-fold, and that of *OsPAO2* was down-regulated (Fig. CII-3). Induction profiles of 7 *OsPAO*s in rice seedlings treated by wounding and drought was quite similar; i.e., *OsPAO2* and *OsPAO6* transcripts accumulated maximally ~50 (drought) to 100-folds (wounding) and ~500 (wounding) to ~700-fold (drought) levels, respectively (Fig. CII-3). High salt treatment induced the quite similar induction patterns on *OsPAO*s as the wounding and drought treatments induced.

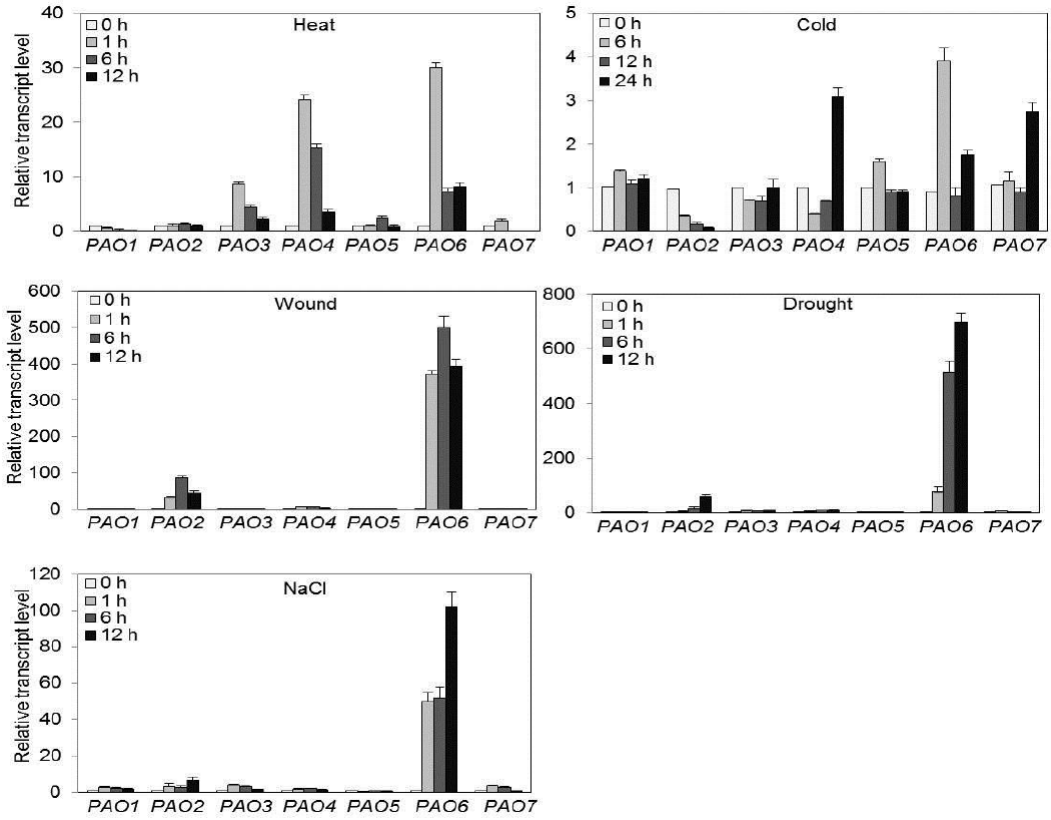

Fig. CII-3. Effect of abiotic stresses on the *OsPAO* expression.

The maximum induction of *OsPAO6* were ~100-fold levels in NaCl stress, which was different from those (400~700-fold levels) in wounding and drought stresses (Fig. CII-3).

Expressional change of *OsPAO*s to reactive oxygen species

Next I tested the effect of hydrogen peroxide (H_2O_2) and methyl viologen (MV) on *OsPAO*s. The former induced *OsPAO6* to ~20-35-fold levels compared to that of control (Fig. CII-4, left). MV modulated the *OsPAO* expression but the respective changes were less than 2-fold increase or less than 0.1-fold decrease (Fig. CII-4, right).

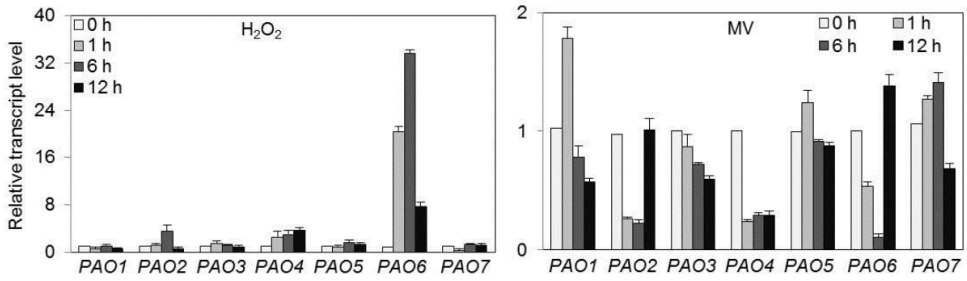

Fig. CII-4. Effect of H_2O_2 and MV on the *OsPAO* expression.

Expressional change of *OsPAO*s to PAs

Lastly I examined the effect of PAs on *OsPAO*s. In Put application, *OsPAO2, OsPAO3*, *OsPAO4, OsPAO6* and *OsPAO7* were induced transiently ~2-fold to 7-fold. The other PAs, Spd, Spm and T-Spm, had inducing effect on *OsPAO2*, *OsPAO6* and *OsPAO7*. The *OsPAO6* transcripts accumulated to ~120-fold levels by Spd, ~250-fold levels by Spm and ~220-fold levels by T-Spm, respectively (Fig. CII-5). *OsPAO2* and *OsPAO7* transcripts also accumulated by those PAs but their maximum levels were less than 20-fold (Fig. CII-5).

Expression profiles of *OsPAO6* and *OsPAO7* in flower organs

Liu et al. (2014b) reported that *OsPAO7* expressed in anther walls and pollens of *O. sativa* flowers. Therefore, I addressed whether *OsPAO6* expresses in flower organs. I collected two stages of *O. sativa* flowers; the one is early+mid phase, and the other is late phase. In early+mid phase, *OsPAO6* was expressed at almost null levels while *OsPAO7* was expressed at moderate levels (Fig. CII-6). In contrast, *OsPAO6* expressed at the higher levels in relative to that of *OsPAO7* in early+mid phase, whereas *OsPAO7* expressed at the decreased levels compared to that of early+mid phase of *OsPAO7* (Fig.

CII-6).

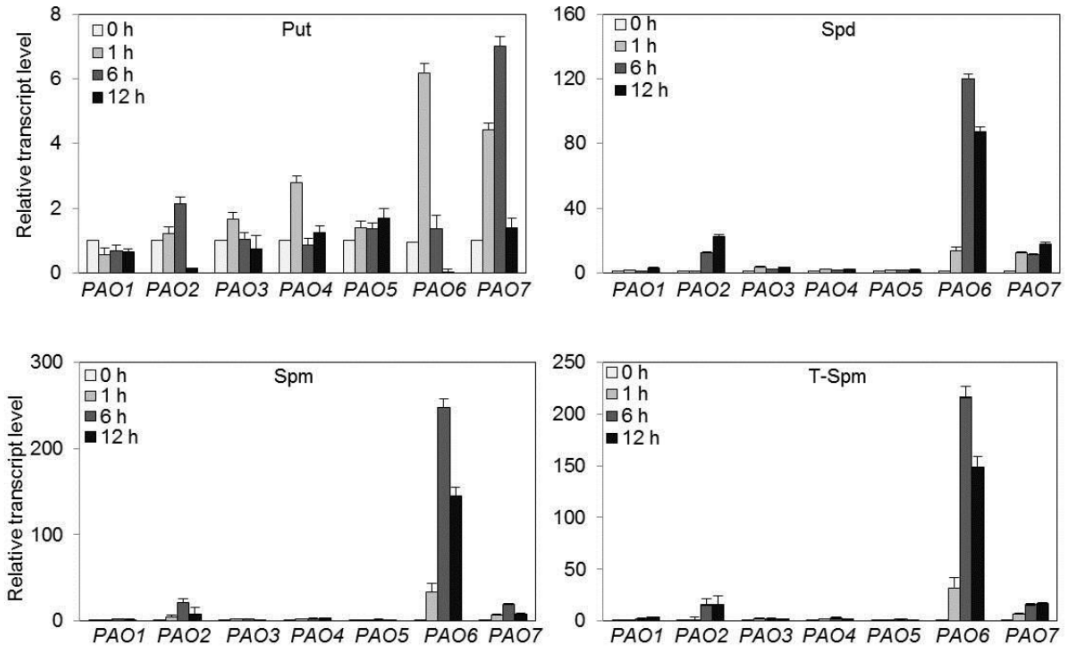

Fig. CII-5. Effect of PAs on the *OsPAO* expression.

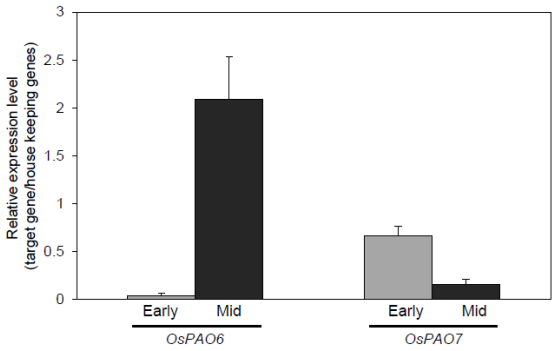

Fig. CII-6. Differential expression of *OsPAO6* and *OsPAO7* in *O. sativa* flower organs.

Chapter summary

In this chapter, I investigated the expressional changes of *OsPAO*s in response to hormones, PAs, oxidative stresses, and abiotic stresses. The induction profiles of 7 *OsPAO*s were summarized in Table CII-3. OsPAO2, OsPAO6 and OsPAO7 are the clade II members. The *OsPAO* genes encoding those clade II members were in common responsive to JA, PAs except diamine, Put, wounding, drought and NaCl stresses. OsPAO3, OsPAO4 and OsPAO5 are the clade IV members, which reside in peroxisomes and function in the BC pathway (Ono et al., 2012). The corresponding genes seemed to be constantly expressed under application of hormones, PAs and ROS, respectively. Of them, *OsPAO3* and *OsPAO4* but not *OsPAO5* were induced mildly upon heat, wounding and drought. OsPAO1 is the clade III member. OsPAO1 localizes in cytoplasm and functions in the BC pathway (Liu et al., 2014a). *OsPAO1* expression was not much modulated by hormones, ROS and abiotic stresses which I tested in this study

Table CII-3. The responsiveness of OsPAOs to hormones, polyamines, oxidative stresses and abiotic stresses. The degreee of the induction was distinctly displayed as + to ++++.
+, 5~10-fold induction; ++, 10~50; +++, 50~100; ++++, >100, respectively.

	Hormones						Polyamines				Oxidative stresses		Abiotic stresses				
	IAA	iP	GA	ABA	JA	SA	Put	Spd	Spm	T-pm	H_2O_2	MV	Heat	Cold	Wounding	Dehydration	NaCl
OsPAO1		+															
OsPAO2					+++			++	++	++					++	++	+
OsPAO3													+			+	
OsPAO4													++		+	++	
OsPAO5																	
OsPAO6					+++		+	++++	++++	++++	+++		++		++++	++++	++++
OsPAO7		++			++		+	++	++	++						+	

I also determined the kinetic parameters of the recombinant OsPAO3, OsPAO4 and OsPAO5 proteins. In Table CII-5, I summarized the kinetic parameters for the optimum PA substrate of the respective OsPAOs. From the *k*cat/*K*m values, the increasing order is OsPAO3=OsPAO4<OsPAO5<OsPAO1<OsPAO7. The first three OsPAOs are the peroxisomal enzymes. I could speculate that the peroxisomal PAO enzymes

back-convert either Spm to Spd or Spd to Put mildly. OsPAO7 functions in the TC pathway. The catalytic efficiency of OsPAO7 was markedly higher compared to those of the clades III and IV.

Table CII-5. Comparison of the kinetic parameters of 5 *O. sativa* PAOs. The values of OsPAO1 and OsPAO7 were cited from the articles of Liu et al. (2014a) and Liu et al. (2014b).

	Clade III, Back conversion	Clade II, Terminal catabolism	
	OsPAO1	OsPAO6	OsPAO7
	T-Spm (pH 6.0)		Spm (pH 6.5)
kcat(s^{-1})	0.051±0.002		32.6±1.2
Km(μM)	3.693±0.229		38.3±2.5
kcat/Km ($M^{-1}s^{-1}$)	13,688±72		853.9±71.4(x10^3)

	OsPAO3	OsPAO4	OsPAO5
	Spd (pH 8.5)	Spm (pH 7.0)	Spm (pH 7.5)
kcat(s^{-1})	0.442±0.138	0.279±0.088	0.629±0.305
Km(μM)	156±37.7	105±25.2	133±25.4
kcat/Km ($M^{-1}s^{-1}$)	2,897±867	2,600±349	4,430±1,765

Clade IV, Back conversion

Chapter III

Characterization of a clade III polyamine oxidase in *Selaginella lepidophylla*

Introduction

As mentioned, in angiosperms, major common PAs are Put, Spd, Spm and T-Spm (Knott et al. 2007; Takahashi and Kakehi 2010; Takano et al. 2012). NorSpd and NorSpm occur in Bryophyta, mosses and some eukaryotic algae (Hamana et al. 1985, 2004; Kuehn et al. 1990). In 1988, NorSpd and NorSpm were detected in alfalfa (Rodoriguez-Garay et al. 1988). The biosynthesis of those uncommon PAs begins with 1,3-diaminopropane (DAP), which is generated by the action of a TC-type of PAO on Spd and Spm (Kusano et al. 2015). The aminopropyl residue derived from dcSAM is transferred to DAP by a putative aminopropyltransferase (APT) with relaxed substrate specificity, resulting in NorSpd, and subsequently, the second APT action converts NorSpd to NorSpm (Fuell et al. 2010).

In this chapter, I isolated the clade III PAO gene (named *SelPAO5*) from a lycophyte, *Selaginella lepidophylla*, which shows the highest sequence identity to *AtPAO5* (Ahou et al. 2014; Kim et al. 2014) and *OsPAO1* (Liu et al. 2014a, 2014c). The recombinant SelPAO5 prefers Spm and T-Spm as substrates to convert to Spd and NorSpd, respectively. The results of my study reveal a novel route for generating NorSpd, and also show that SelPAO5 oxidizes T-Spm at a different carbon position than AtPAO5 and OsPAO1 in angiosperms.

Results

Identification of *SlPAO5*, the clade III PAO from *S. lepidophylla*

My colleagues recently characterized *AtPAO5* and *OsPAO1* (Kim et al. 2014; Liu et al. 2014a). Although I proposed that the products of these genes, AtPAO5 and OsPAO1, function as T-Spm oxidases, because the loss-of-function mutant of *AtPAO5* specifically accumulates twice as much T-Spm as WT plants, both of the recombinant enzymes prefer Spm and T-Spm *in vitro* and back-convert them to Spd (Kim et al. 2014; Liu et al. 2014a; Liu et al. 2014b). Considering the phylogeny of plants (Bowman et al. 2007), I found *AtPAO5* orthologs in the lycophyte *Selaginella moellendorffii* (Banks et al. 2011) but not in bryophytes such as *Marchantia polymorpha* and *Physcomitrella patens* (DW Kim, personal communication; Fig. CIII-1A). Based on this information, I tried to isolate *AtPAO5* ortholog(s) from *S. lepidophylla*. I designed a primer pair based on *SmPAO6* and *SmPAO7* cDNA sequences (Accession numbers XP_002984796.1 and XP_002985859.1) from *S. moellendorffii* (Table CIII-1). PCR amplification using this primer pair and *S. lepidophylla* genomic DNA resulted in a 813-bp fragment that showed 62% and 61% identity to *SmPAO6* and *SmPAO7* cDNAs, respectively. Next, I performed inverse-PCR (http://labs.mcdb.lsa.umich.edu/labs/maddock/ protocols/PCR/ inverse_pcr _protocol.html) of *S. lepidophylla* genomic DNA using two pairs of primers. The genome template was prepared as follows: *S. lepidophylla* genomic DNA was digested with either *Hin*dIII or *Sal*I and then self-ligated according to the protocol. The resulting fragments were sequenced and a 1584-bp open-reading frame (ORF) was identified. Based on the results of RT-PCR of total RNA prepared from *S. lepidophylla* using a new primer pair covering the above ORF, I confirmed that this ORF is the correct one, and I designated the corresponding transcript *SelPAO5* (accession number LC036642). *SelPAO5* is intron-less, which is consistent with the gene structures of *SmPAO6*, *SmPAO7*, *AtPAO5* and *OsPAO1* (Kim et al. 2014; Liu et al. 2014a). The translation product of *SelPAO5* is a 527-amino acid protein, which I designated SelPAO5. I generated a phylogenetic tree using the sequences of SelPAO5, seven *O. sativa* PAOs, five *A. thaliana* PAOs, eight *S. moellendorffii* PAOs and several other angiosperm PAOs. Based on this tree, SelPAO5 is classified in clade III (Fig. CIII-1B).

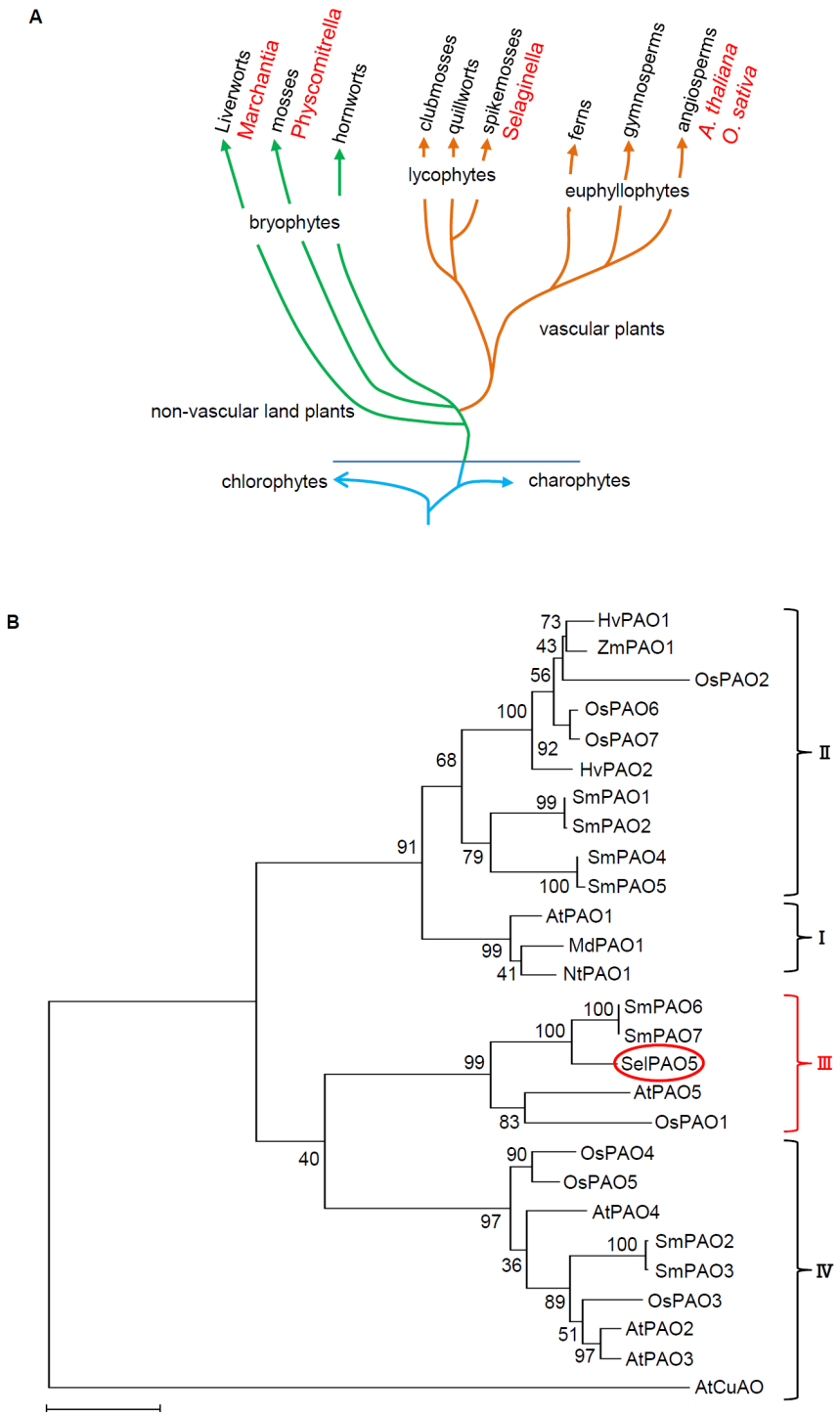

Fig. CIII-1. Classification of SelPAO5 from *S. lepidophylla* in the phylogeny of plant PAOs . **A**. Phylogenic relationship between spikemosses and angiosperms in the plant kingdom. **B**. Phylogenetic tree of SelPAO5, other *Selaginella* PAOs and selected angiosperm PAOs. The amino acid sequences of SelPAO5, eight PAOs from *S. moellendorffii* and several PAOs from angiosperms were subjected to phylogenetic analysis. The maximum likelihood tree was built by alignment of the amino acid sequences of PAOs and Arabidopsis copper-dependent amine oxidase 1 (as an outgroup) using Molecular Evolutionary Genetics Analysis (MEGA) software version 6.0 [21]. Bootstrap values obtained with 1,000 replicates are indicated at the nodes. Roman numerals (I–V) indicate clade numbers. The genes and accession numbers used are as follows: SelPAO5 (LC036642), SmPAO1 (XP_002965265.1), SmPAO2 (XP_002965599.1), SmPAO3 (XP_002968082.1), SmPAO4 (XP_002969966.1), SmPAO5

(XP_002981437.1), SmPAO6 (XP_002984796.1), SmPAO7 (XP_002985859.1), SmPAO8 (XP_002986593.1), OsPAO1 (NM_001050573), OsPAO2 (NM_001055782), OsPAO3 (NM_001060458), OsPAO4 (NM_001060753), OsPAO5 (NM_001060754), OsPAO6 (NM_001069545), OsPAO7 (NM_001069546), AtPAO1 (NM_121373), AtPAO2 (AF364952), AtPAO3 (AY143905), AtPAO4 (AF364953), AtPAO5 (AK118203), ZmPAO1 (*Zea mays* PAO1, NM_001111636), NtPAO1 (*Nicotiana tabacum* PAO, AB200262), HvPAO1 (*Hordeum vulgare* PAO1, AJ298131), HvPAO2 (*Hordeum vulgare* PAO2, AJ298132), and MdPAO1 (*Malus domestica* PAO, AB250234).

Subcellular localization of SelPAO5 in plant cells

Subcellular localization of SelPAO5 was addressed by the GFP fusion method. The fusion construct was delivered into onion epidermal cells by particle bombardment (PDS-1000/He, Bio-Rad). The green fluorescent signal from the construct seemed to be of cytoplasmic origin (Fig. CIII-2) as similar as that of the GFP control construct (data not shown).

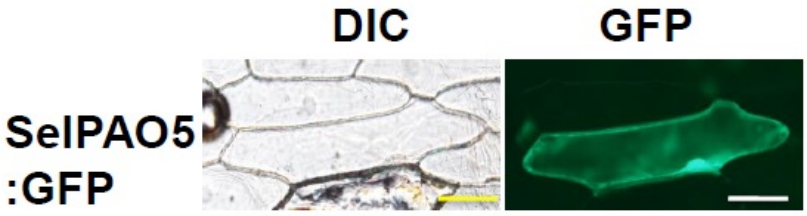

Fig. CIII-2. Subcellular localization of SelPAO5 in plant cells. Bar corresponds to 10 μm.

Enzymatic characteristics of the recombinant SelPAO5

The recombinant SelPAO5 protein was homogenously purified (Fig. CIII-3A). The absorbance spectrum shows that the purified enzyme has two peaks at approximately 380 and 460 nm, which is indicative of the association of flavin adenine dinucleotide with the enzyme (Fig. CIII-3B). The optimal pH and temperature for maximum SelPAO5 activity using Spm as a substrate were pH 8.0 and 30°C, respectively (Fig. CIII-3C and 3E). The maximum SelPAO5 activity with T-Spm as a substrate occurred at pH 7.0 and at a temperature of 35°C (Figs. CIII-3D, 3F). As SelPAO5 activity was highest at pH 8.0 for Spm and pH 7.0 for T-Spm (Figs. CIII-3C and 3D), we examined recombinant SelPAO5 substrate specificity at pH 8.0 and pH 7.0 using 300 μM substrate. At pH 8.0, the substrate preference of SelPAO5 in decreasing order was as follows: Spm = T-Spm > N^1-acetyl Spm > NorSpm > Spd (Fig. CIII-4A). At pH 7.0, the substrate preference of SelPAO5 in decreasing order was as follows: T-Spm > NorSpm

> Spm > N^1-acetyl Spm > Spd (Fig. CIII-4B). At both pH levels, SelPAO5 catalyzed Spd at a very low rate (Figs. CIII-4A, 4B, 5B).

SelPAO5 back-converts Spm to Spd and T-Spm to NorSpd

We analyzed the reaction product(s) of Spm and T-Spm catalyzed by SelPAO5. Using Spm as a substrate, Spd was produced in a time-dependent manner (Fig. CIII-4C), indicating that SelPAO5 catabolizes Spm in a back-conversion pathway, same as AtPAO5 and OsPAO1 (Kim et al. 2014; Liu et al. 2014a). Unexpectedly, when T-Spm was used as a substrate, the peak, which appears to correspond to NorSpd, increased in a time-dependent manner at both pH 7.0 and pH 8.0 (Figs. CIII-4D, 5B). To verify our prediction, the peak fraction was subjected to LC-MS/MS analysis along with tri-benzoylated NorSpd (Fig. CIII-6) as a standard. The candidate chemical was clearly identified as NorSpd (Fig. CIII-7).

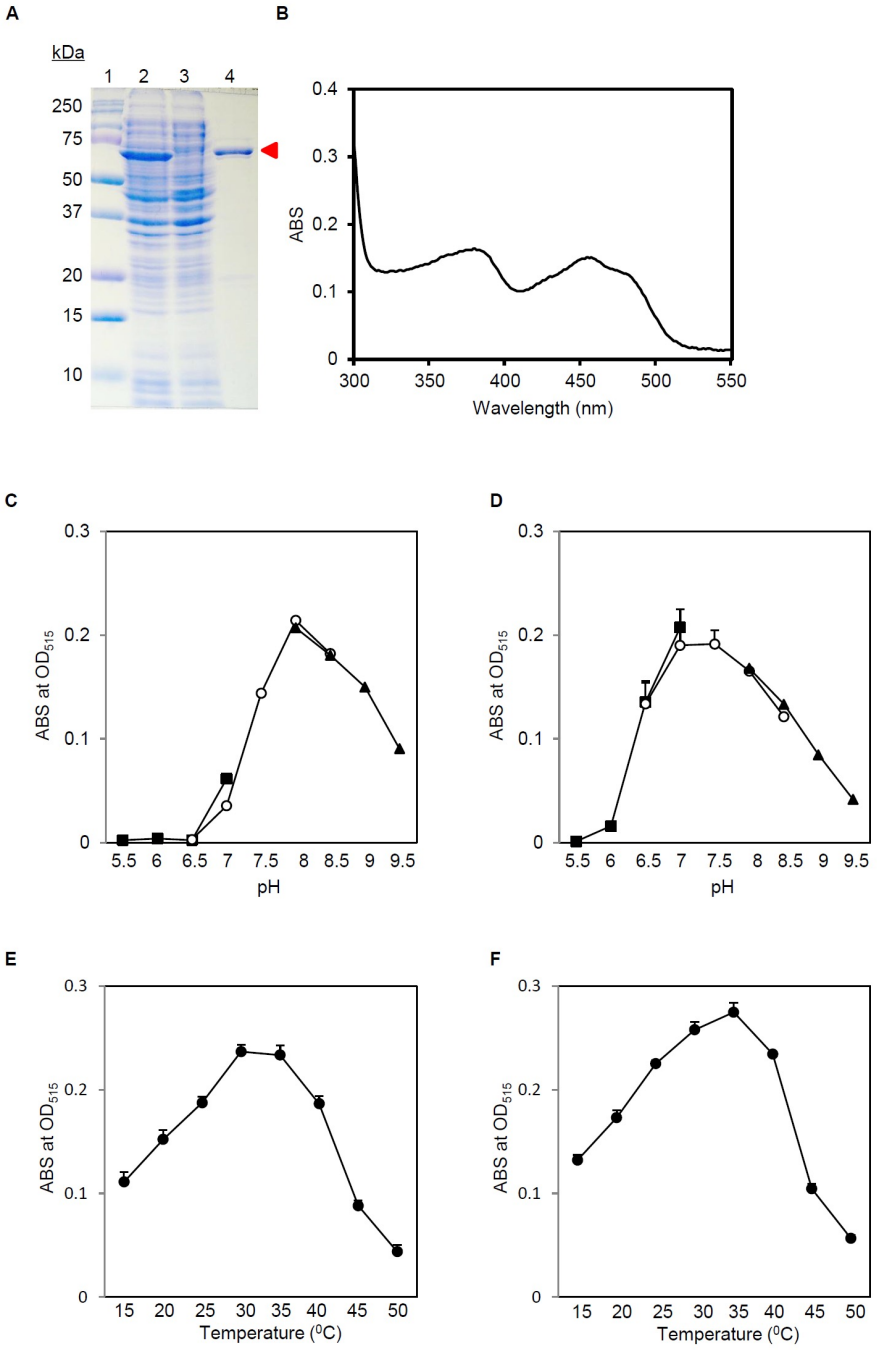

Fig. CIII-3. Characterization of recombinant SelPAO5. **A**, Purification of SelPAO5. Lane 1, Molecular size marker; lane 2, IPTG-induced crude extract after sonication; lane 3, non-induced crude extract after sonication; lane 4, SelPAO5 purified by Ni-affinity chromatography (25-fold concentrated sample compared with that of lanes 2 and 3). **B**, Absorbance spectrum of purified sample ranging from 300 nm to 550 nm. C, Optimal pH for SelPAO5 activity using Spm as substrate. The buffers used are as follows: pH 5.5 to 7.0, 100 mM MES buffer (■), pH 6.5 to 8.5, 100 mM HEPES buffer (○), pH 8.0 to 9.5, 100 mM Tricine buffer (▲). **D**, Optimal pH for SelPAO5 activity with T-Spm as substrate. **E**, Optimal temperature for SelPAO5 activity with Spm as substrate at pH 8.0. **F**, Optimal temperature for SelPAO5 activity with T-Spm as substrate at pH 7.0.

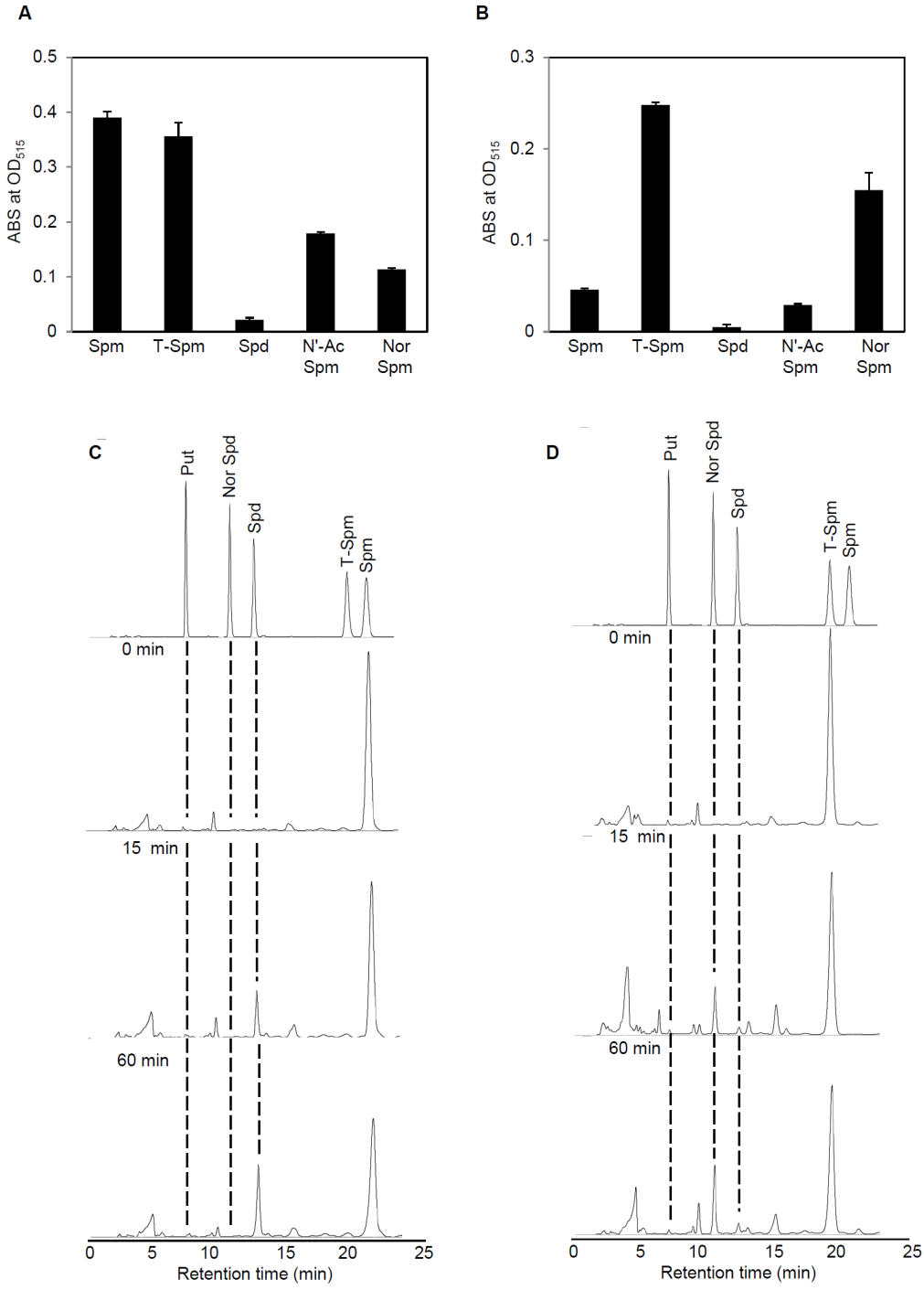

Fig. CIII-4. Substrate specificity of recombinant SelPAO5 and SelPAO5-catalyzed reaction product(s) of T-Spm and Spm. The enzymatic activity of recombinant SelPAO5 was determined in 100 mM HEPES buffer at pH 8.0 (**A**) and 100 mM MES pH 7.0 (**B**) at 35°C. **A** and **B**, Substrate (500 µM each) was incubated at 35°C for 10 min, and the resulting production of H_2O_2 was measured. Enzyme activity is displayed as relative Abs at 515 nm. The experiments were repeated at least three times, and the mean ± SD values are displayed. **C**. HPLC analysis after conversion of Spm at pH 8.0. **D**, HPLC analysis after conversion of T-Spm at pH 7.0. **C** and **D**, top panels, PA (Put, NorSpd, Spd, T-Spm, and Spm) standard; second, third and bottom panels show product analysis after 0, 15 and 60 min incubation with SelPAO5, respectively.

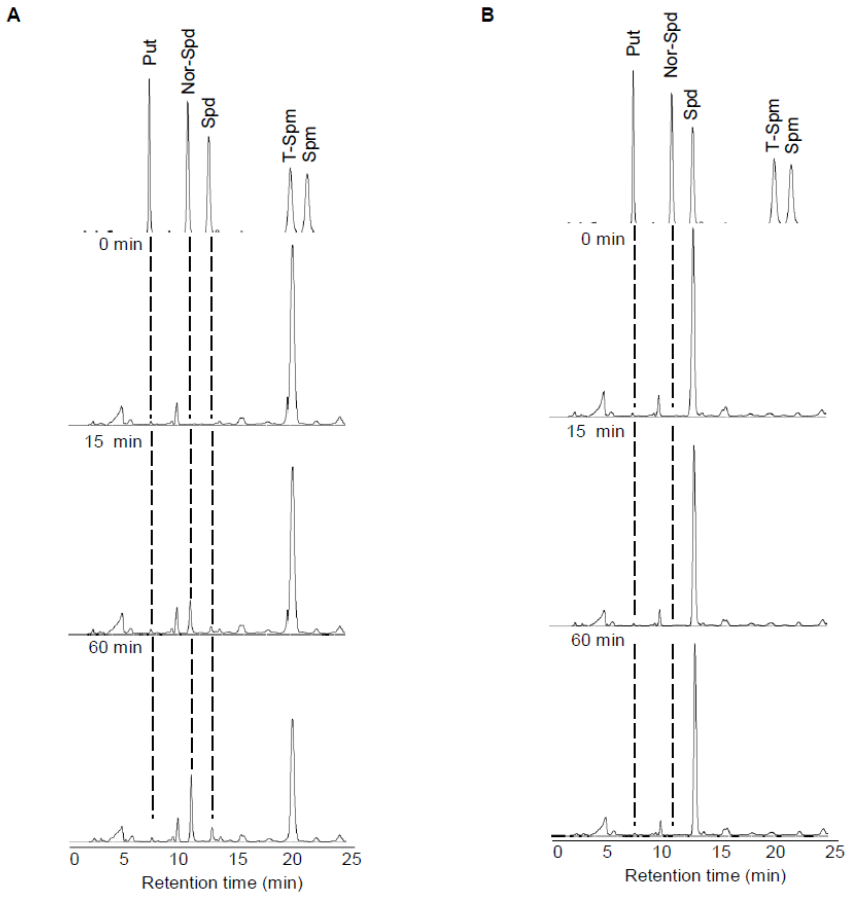

Fig. CIII-5. HPLC analysis of the reaction product(s) of T-Spm (A) and Spd (B) catalyzed by SelPAO5 at 100 mM HEPES buffer (pH 8.0). A, B. top panels, PA (Put, NorSpd, Spd, T-Spm, and Spm) standard; second, third and bottom panels show product analysis after 0, 15 and 60 min incubation with SelPAO5, respectively.

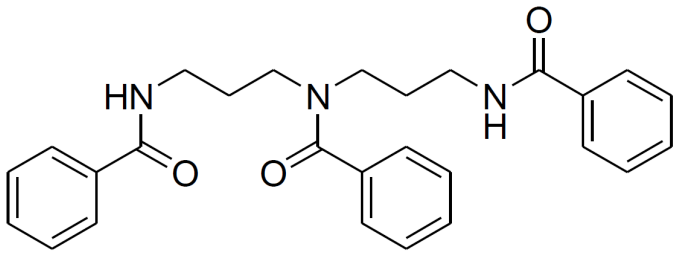

Fig. CIII-6. Structure of tri-benzoylated Norspermidine.

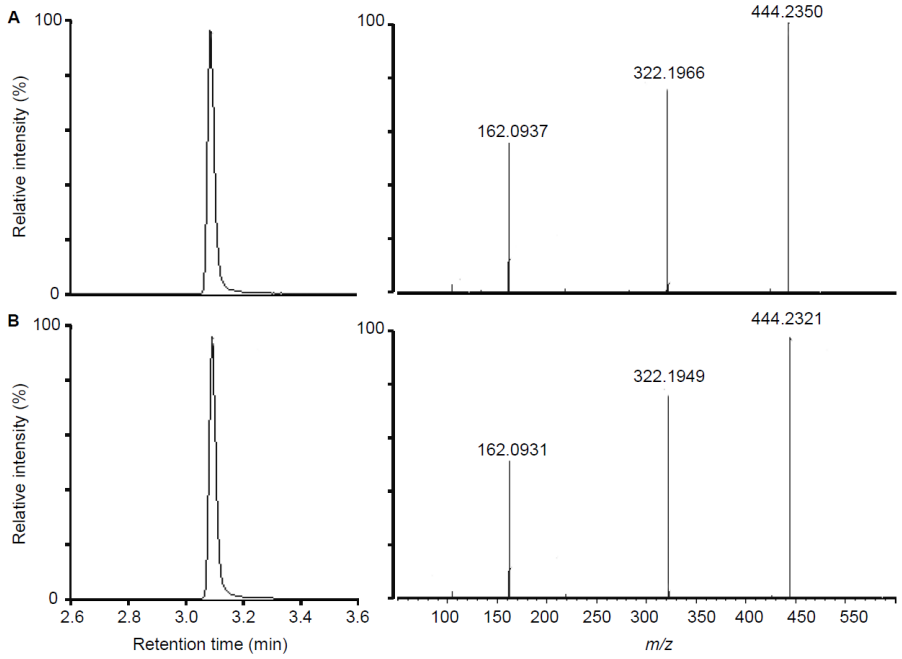

Fig. CIII-7. Identification of NorSpd as the reaction product of T-Spm oxidation by SelPAO5. **A**. LC-MS/MS analysis of tri-benzoylated NorSpd (standard). Selected reaction monitoring (Left) and full-scan spectra of fragment ions (Right) of authentic NorSpd. **B**. LC-MS/MS analysis of the benzoylated reaction product of T-Spm oxidation by SelPAO5. Selected reaction monitoring (Left) and full-scan spectra of fragment ions (Right).

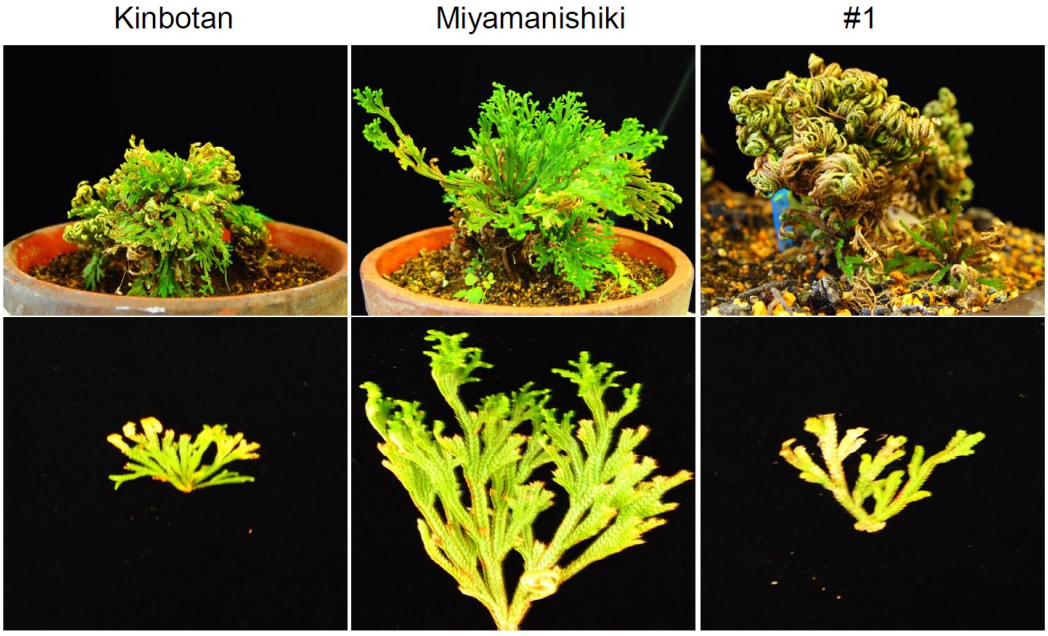

Fig. CIII-8. Three Selaginella varieties obtained from a professional gardener, Mr. Kiyoshi Ishikawa. Upper: whole plants; lower: leaflet. #1 has no-name.

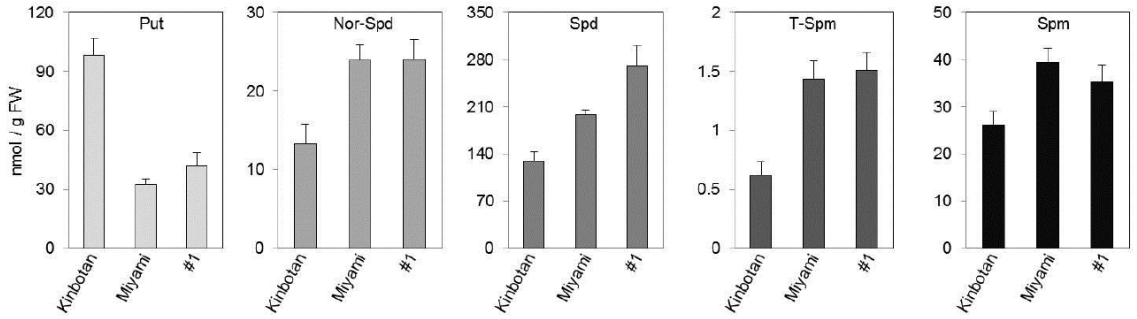

Fig. CIII-9. PA composition in three *Selaginella* varieties.

Selaginella plants contain NorSpd as well as four common PAs

Next, I obtained three *Selaginella* varieties (see Fig. CIII-8) and analyzed their PA composition. These *Selaginella* plants contained Put, Spd and Spm at levels greater than 25 nmol/g fresh weight (FW) (Fig. CIII-9). Interestingly, the NorSpd content was greater than 10 nmol/g FW, whereas the T-Spm content was less than one-tenth that of NorSpd and Spm (Fig. CIII-9). As one of the unique features of the *Selaginella* genus is tolerance to desiccation (Banks et al. 2011; Friedman 2011; Yobi et al. 2012), I examined the effect of dehydration stress on PA contents in *Selaginella* plants. The levels of Put, NorSpd, Spd and Spm contents increased significantly after dehydration treatment, whereas that of T-Spm did not change or decreased compared to that of well-watered leaflet (Fig. CIII-9).

Expression of *SelPAO5* is down-regulated by dehydration stress and up-regulated by T-Spm treatment

I then addressed whether *SelPAO5* is responsive to dehydration stress. The levels of *SelPAO5* transcripts decreased distinctly after dehydration stress (Fig. CIII-10A). To find a clue of the SelPAO5 function, I tested the levels of *SelPAO5* transcripts after Spm- and T-Spm- treatment and found that the *SelPAO5* transcripts markedly accumulated by T-Spm treatment but not much by Spm treatment (Fig. CIII-10B).

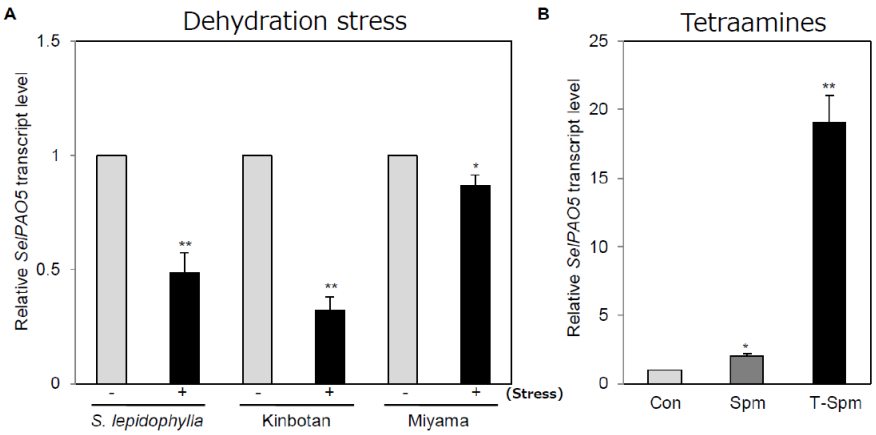

Fig. CIII-10. Effect of dehydration stress (A) and tetraamine treatment (B) on the expression of *SelPAO5*.

Chapter summary

I showed that the *Selaginella* plants contained NorSpd at levels of over 10 nmol/g FW and T-Spm levels of only one-tenth of NorSpd. The *S. moellendorffii* genome contains a putative T-Spm synthase gene (Banks et al., 2011). The recombinant SelPAO5 catalyzes the conversion of T-Spm to NorSpd. Based on the results, I propose that NorSpd is generated via T-Spm catabolism by SelPAO5. As previously mentioned, NorSpd and NorSpm are synthesized by the sequential transfer of the aminopropyl residue to DAP (Rodriguez-Garay et al., 1988; Fuell et al., 2010). The latter is formed by the action of a terminal catabolism-type PAO (Kusano et al., 2015). Therefore, the route from T-Spm to NorSpd catalyzed by PAO is a novel PA metabolic pathway.

T-Spm is an asymmetric isomer of Spm, which has a symmetrical structure. Here, I tentatively numbered the carbon atoms of T-Spm C_1 to C_{10} (Fig. CIII-11). AtPAO5 and OsPAO1 prefer Spm and T-Spm *in vitro* and produce Spd from both of these substrates (Liu etal., 2014a; Ahou et al., 2014; Kim et al., 2014), indicating that both enzymes oxidize the C_3-carbon. Unlike these enzymes, SelPAO5 produces NorSpd from T-Spm, indicating that SelPAO5 oxidizes the C_7-carbon of T-Spm (Fig. CIII-11).

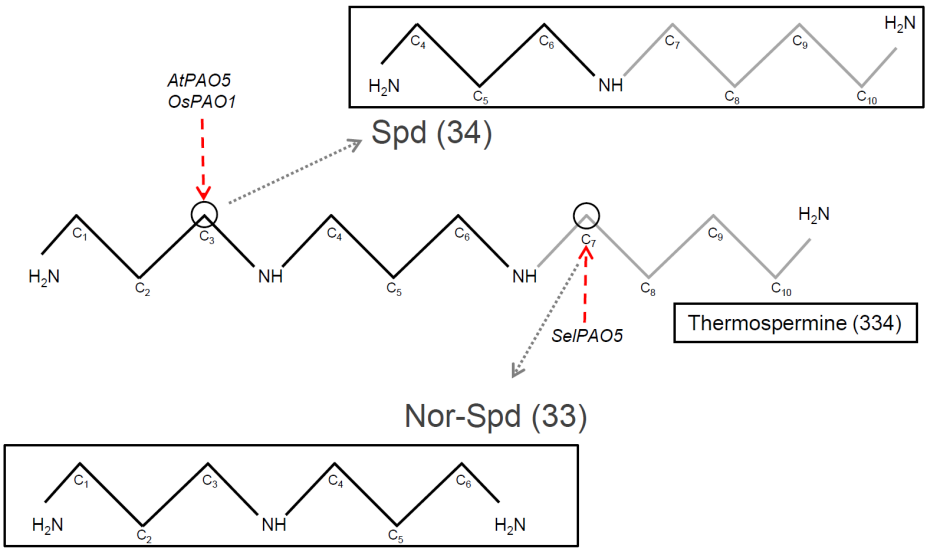

Fig. CIII-11. SelPAO5 oxidizes the C_7-carbon of T-Spm whereas AtPAO5 and OsPAO1 oxidize its C_3-carbon.

Discussion

In this thesis study, I isolated the 6th PAO (*OsPAO6*) gene of rice (chapter I). The deduced amino acid sequence of OsPAO6 shows high levels (92%) of identity to that of OsPAO7. The former is a 497-amino acid-protein, and the latter is a 474-amino acid-protein. My preliminary result indicated that OsPAO6 generates DAP from Spd and Spm, suggesting that OsPAO6 functions in the TC pathway. This protein localizes in the apoplast as same as OsPAO7. Therefore, OsPAO6 and OsPAO7 seem to be cognate proteins.

I also performed the expression analysis of the 7 *OsPAO*s in this study (chapter II), and found that the clade II *OsPAO* member genes, *OsPAO2*, *OsPAO6* and *OsPAO7*, are responsive to JA and PA treatments, and that *OsPAO2* and *OsPAO6* are also responsive to abiotic stresses (Table CII-3). Involvement of JA in wounding and drought stresses is well established (Creelman and Mullet 1995; Turner et al., 2002; Wasternack et al., 2006; Song et al., 2014). Hydrogen peroxide but not MV was able to induce *OsPAO6* but not *OsPAO2* and *OsPAO7*. I should refer that the degree of *OsPAO2*- and *OsPAO6* induction is different; for example, in wounding, *OsPAO6* transcripts reached to ~500-fold levels, while *OsPAO2* transcripts reached to ~100-fold levels compared to controls. The difference may be explained that the *OsPAO2* expression is simply regulated by JA, whereas the *OsPAO6* expression is synergistically regulated by JA, H_2O_2, PAs and/or unidentified factor(s). Maize PAO (ZmPAO) was reported to be involved in wound healing (Cona et al., 2006; Angelini et al., 2008). Those authors further showed that H_2O_2 produced by ZmPAO plays a critical role in peroxidase-mediated wall stiffening events because inhibition of ZmPAO, by a specific inhibitor, resulted in the strongly reduced lignin and suberin deposition along the wound (Kolattukudy 1981; Angelini et al., 2008; Weng and Chapple 2010). Even in flower organ, timing of expression of *OsPAO6* and *OsPAO7* differed. Namely *OsPAO7* preceded expression of *OsPAO6* (Fig. CII-6). In Arabidopsis, JA signaling is essential for late stamen development (Sanders et al., 2000; Song et al., 2013). The knowledge of stamen development extended to *O. sativa* and the similarity on the basal knowledge was confirmed (Wilson and Zhang 2009). Arabidopsis mutants deficient in JA signaling components, and the transgenic plants overexpressing jasmonate zim-domain proteins (JAZs) became male-sterile due to failure of filament elongation, delayed anther dehiscence (Song et al., 2013). As *OsPAO6* was JA-responsive, the expressional difference of *OsPAO6* and *OsPAO7* in flower organs may be explained again by the control of JA. I am interested in the phenotypes of the mutants of the

respective *OsPAO* genes, especially the *Ospao6* mutant.

Furthermore I determined the kinetic parameters of the recombinant OsPAO3, OsPAO4 and OsPAO5 (chapter II), and compared those of other OsPAO members, OsPAO1 (Liu et al., 2014a) and OsPAO7 (Liu et al., 2014b). The catalytic efficiency (k_{cat}/K_m) values of OsPAO3, OsPAO4 and OsPAO5 were in the range of 2.6~4.4 x10^3 $M^{-1}s^{-1}$ (Fig. D-1). *Arabidopsis thaliana* has 5 PAO genes, and the 3 gene products (AtPAO2, AtPAO3 and AtPAO4) out of them were classified into the clade IV (Tavladoraki et al., 2006; Kamada-Nobusada et al., 2008; Moschou et al., 2008; Takahashi et al., 2010; Ahou et al., 2014; Kim et al., 2014). The catalytic efficiency values of AtPAO2, AtPAO3 and AtPAO4 were in the range of 15~90 x10^3 $M^{-1}s^{-1}$ (Fincato et al., 2011) and quite comparable to those of OsPAO3, OsPAO4 and OsPAO5. This is reasonable because those peroxisomal PAO members contribute to PA homeostasis even though their PA specificity differs respectively. The k_{cat}/K_m values of OsPAO1 were 7~13 x 10^3 $M^{-1}s^{-1}$ (Liu et al., 2014a). Another unique feature is that it has a low K_m. As OsPAO1 and the Arabidopsis ortholog, AtPAO5, are suggested to function as a T-Spm oxidase (Kim et al., 2014; Liu et al., 2014c) and the T-Spm contents in the organisms are quite low compared to those of other PAs, this fits well to the situation in the organisms.

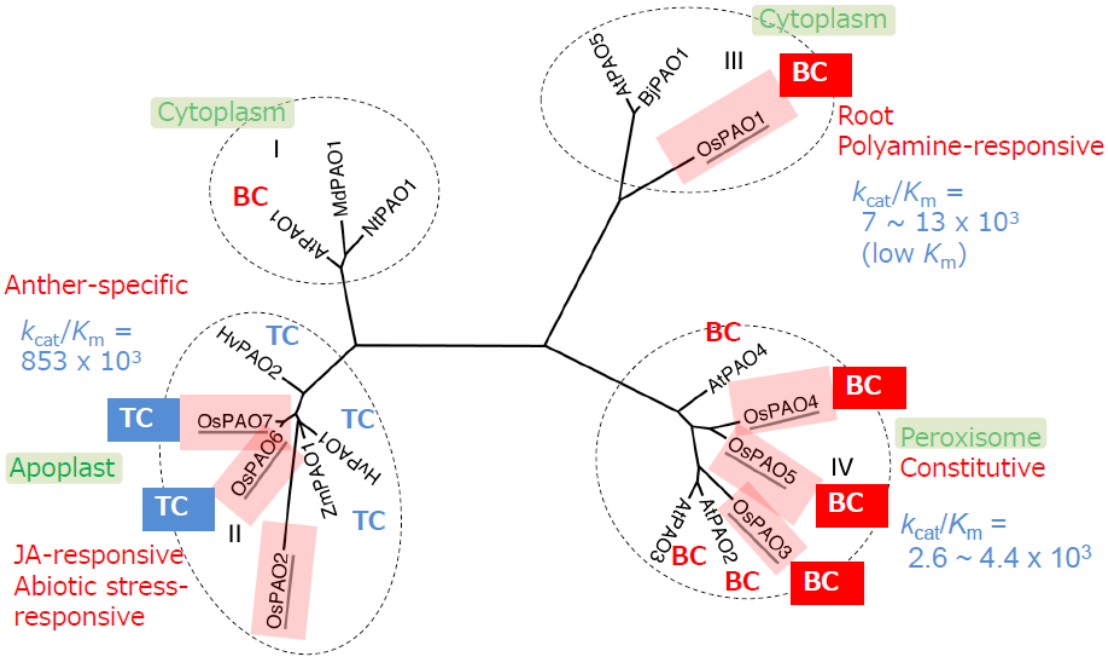

Fig. D-1. Summary of PAOs in *O. sativa*.

At this moment, I could not purify the recombinant OsPAO6 and, therefore, could not

get the kinetic parameter values. The other clade II member, OsPAO7, showed the k_{cat}/K_m values were 853 x 10^3 $M^{-1}s^{-1}$. The k_{cat}/K_m values of maize ZmPAO, the clade II member, were reported to be 20 x 10^6 $M^{-1}s^{-1}$ (Fincato et al., 2011). Considering the kinetic values, I can speculate that the function of TC-type PAOs is the supply of H_2O_2 for repairing the wounded portions or stiffening events of the cell walls under normal growth.

In the last chapter, I isolated the clade III PAO member, *SelPAO5*, from *S. lepidophylla* and characterized it. Of interest, the gene product, SelPAO5, produced NorSpd from T-Spm and Spd from Spm, respectively. Spm has a symmetric structure of C3C4C3, while T-Spm is an asymmetric structure of C3C3C4 (see Introduction). Angiosperms' the clade III PAOs such as AtPAO5 and OsPAO1 produced Spd from both Spm and T-Spm (Ahou et al., 2014; Liu et al., 2014a; Kim et al., 2014), indicating that both enzymes oxidize the C_3-carbon of T-Spm, whereas SelPAO5 oxidizes the C_7-carbon of T-Spm (Fig. CIII-11). PAO-mediated NorSpd production is a novel route for NorSpd synthesis. From an evolutional point of view, I could guess that the clade III PAO was adapted to recognize the C_3-carbon position instead of C_7-carbon during the process of evolution from Selaginella to angiosperms, rice and Arabidopsis.

Actually Selaginella plants contained NorSpd at levels of over 10 nmol/g FW, whereas the levels of T-Spm were one-tenth of NorSpd. The *S. moellendorffii* genome contains a putative T-Spm synthase gene (Banks et al., 2011)

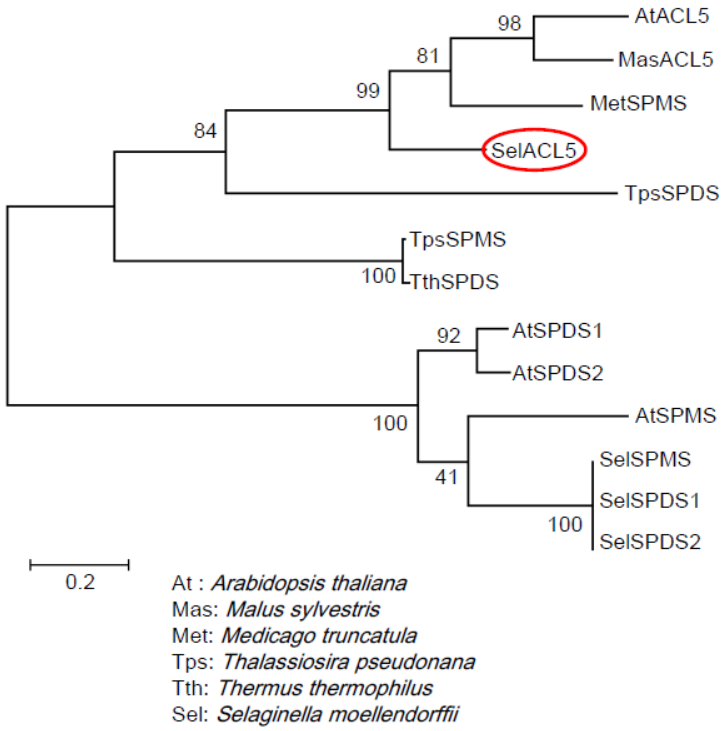

Fig. D-2. Phylogenetic tree of T-Spm synthase genes. The numbers at the nodes indicate the bootstrap values based on maximum likelihood (MEGA) algorithms with 1,000 replications.

(Fig. D-2). Furthermore, the expression of *SelPAO5* was significantly induced by exogenously applied T-Spm. Taken together, I could speculate that T-Spm, produced by Selaginella ACL5, is highly toxic to Selaginella, and to reduce its toxicity, SelPAO5 catabolizes T-Spm to NorSpd, which is less toxic.

References

Ahou A, Martignago D, Alabdallah O, Tavazza R, Stano P, Macone A, Pivato M, Masi A, Rambla JL, Vera-Sirera F, Angelini R, Federico R, Tavladoraki P. (2014) A plant spermine oxidase/dehydrogenase regulated by the proteasome and polyamines. *Journal of Experimental Botany* 65:1585-1603.

Alcázar R, Altabella T, Marco F, Bortolotti C, Reymond M, Koncz C, Carrasco P, Tiburcio AF. (2010) Polyamines: molecules with regulatory functions in plant abiotic stress tolerance. *Planta* 231:1237-1249.

Apel K, Hirt H. (2004) Reactive oxygen species: metabolism, oxidative stress, and signal transduction. *Annual Review of Plant Biology* 55: 373-399

Angelini R, Cona A, Federico R, Fincato P, Tavladoraki P, Tisi A. (2010) Plant amine oxidases "on the move": an update. *Plant Physiology and Biochemistry* 48:560-564.

Angelini R, Tisi A, Rea G, Chen MM, Botta M, Federico R, Cona A. (2008) Involvement of polyamine oxidase in wound healing. Plant Physiology 146: 162-177.

Bagni N, Tassoni A. (2001) Biosynthesis, oxidation and conjugation of aliphatic polyamines in higher plants. *Amino Acids* 20:301-317.

Banks JA, Nishiyama T, et al. (2011) The Selaginella genome identifies genetic changes associated with the evolution of vascular plants. *Science* 332:960-963.

Berberich T, Sagor GHM, Kusano T. (2015). Polyamines in plant stress response. In *Polyamine: A universal molecular nexus for growth, survival and specialized metabolism*, eds.T. Kusano and H. Suzuki (Springer Tokyo), 155–168.

Binda C, Coda A, Angelini R, Federico R, Ascenzi P, Mattevi A. (1999) A 30 angstrom long U-shaped catalytic tunnel in the crystal structure of polyamine oxidase. *Structure* 7:265-276.

Bolenius FN, Seiler N. (1981) Acetylderivatives as intermediates in polyamine catabolism. *International Journal of Biochemistry* 13:287-292.

Bouchereau A, Aziz A, Larher F, Martin TJ. (1999) Polyamines and environmental challenges: recent development. *Plant Science* 140:103-125.

Bowman JL, Floyd SK, Sakakibara K (2007) Green genes – comparison genomics of the green branch of life. *Cell* 129:229-234.

Creelman RA, Mullet JE. (1995) Jasmonic acid distribution and action in plants: regulation during development and response to biotic and abiotic stress. *Proceedings of the National Academy of Sciences of the United States of America* 92:4114-4119.

Casero RA Jr, Pegg AE. (1993) Spermidine/spermine N1-acetyltransferase – the turning point in polyamine metabolism. *The FASEB Journal* 7:653-661.

Cervelli M, Bianchi M, Cona A, Crosatti C, Stanca M, *et al*. (2006) Barley polyamine oxidase isoforms 1 and 2, a peculiar case of gene duplication. *The FEBS Journal* 273:3990-4002.

Cervelli M, Caro OD, Penta AD, Angelini R, Federico R, Vitale A, Mariottini P. (2004) A novel C-terminal sequence from barley polyamine oxidase is a vacuolar sorting signal. *The Plant Journal* 40:410-418.

Cervelli M, Cona A, Angelini R, Polticelli F, Federico R, Mariottini P. (2001) A barley polyamine oxidase isoform with distinct structural features and subcellular localization. *European Journal of Biochemistry* 268:3816-3830.

Cervelli M, Polticelli F, Federico R, Mariottini P. (2003) Heterologous expression and characterization of mouse spermine oxidase. *The Journal of Biology Chemistry* 278:5271-5276.

Chen J, Acton TB, Basu SK, Montelion GT, Inoue M. (2002) Enhancement of the solubility of proteins overexpressed in *Escherichia coli* by heat shock. *Journal of Molecular Microbiology Biotechnology* 4:519-524.

Clough SJ, Bent AF. (1998) Floral dip: a simplified method for Agrobacterium-mediated transformation of *Arabidopsis thaliana*. *The Plant Journal* 16:735-743.

Cohen SS. (1998) A guide to the polyamines. *Oxford University Press*, Oxford.

Cona A, Federico R, Gramiccia M, Orsini S, Gradoni L. (1991) The amino aldehydes produced by spermine and spermidine oxidation with maize polyamine oxidase have anti-leishmanial effect. *Biotechnology and Applied Biochemistry* 14:54-59.

Cona A, Moreno S, Cenci F, Federico R, Angelini R. (2005) Cellular redistribution of flavine-containing polyamine oxidase in differentiating root and mesocotyl of *Zea mays* L. seedlings. *Planta* 221:265-276.

Cona A, Rea G, Angelini R, Federico R, Tavladoraki P. (2006) Functions of amine

oxidases in plant development and defence. *Trends Plant Science* 11:80-88.

Del Duca S, Beninati S, Serafini-Fracassini D. (1995) Polyamines in chloroplasts: identification of their glutamyl and acetyl derivatives. *Biochemical Journal* 305:233-237.

Eisenberg T, Knauer H, Schauer A, Büttner S, Ruckenstuhl C, Carmona-Gutierrez D, Ring J, Schroeder S, Magnes C, Antonacci L, Fussi H, Deszcz L, Hartl R, Schraml E, Criollo A, Megalou E, Weiskopf D, Laun P, Heeren G, Breitenbach M, Grubeck-Loebenstein B, Herker E, Fahrenkrog B, Fröhlich K-U, Sinner F, Tavernarakis N, Minois N, Kroemer G, Madeo F. (2009) Induction of autophagy by spermidine promotes longevity. *Nature Cell Biology* 11:1305-1314.

Falasca G, Francechetti M, Bagni N, Altamura MM, Biasi R. (2010) Polyamine biosynthesis and control of the development of functional pollen in kiwifruit. *Plant Physiology Biochemistry* 48:565-573.

Federico R, Angelini R. (1991) Polyamine catabolism in plants. In RD Slocum, HE Flores, eds, Biochemistry and Physiology of Polyamines in Plants. *CRC Press, Boca Raton, FL*: pp 41-56.

Federico R, Cona A, Angelini R, Schininà ME, Giartosio A. (1990) Characterization of maize polyamine oxidase. *Phytochemistry* 29:2411-2414.

Federico R, Ercolini L, Laurenzi M, Angelini R. (1996) Oxidation of cetylpolyamines by maize polyamine oxidase. *Phytochemistry* 43:339-341.

Fellenberg C, Ziegler J, Handrick V, Vogt T. (2012) Polyamine homeostasis in wild type and phenolamide deficient *Arabidopsis thaliana* stamens. *Frontiers Plant Science* 3, article 180

Fincato P, Moschou PN, Spedaletti V, Tavazza R, Angelini R, *et al*. (2011) Functional diversity inside the Arabidopsis polyamine oxidase gene family. *Journal of Experimental Botany* 62:1155-1168.

Fincato P, Moschou PN, Ahou A, Angelini R, Roubelakis-Angelakis KA, *et al*. (2012) The members of *Arabidopsis thaliana PAO* gene family exhibit distinct tissue- and organ-specific expression pattern during seedling growth and flower development. *Amino Acids* 42:831-841.

Flores HE, Galston AW. (1982) Analysis of polyamines in higher plants by high performance liquid chromatography. *Plant Physiology* 69:701-706.

Friedman WE. (2011) Plant genomics: homoplasy heaven in a Lycophyte genome. *Current Biology* 21:R554-R556.

Fuell C, Elliot KA, Hanfrey CC, Franceschetti M, Michael AJ. (2010) Polyamine biosynthetic diversity in plants and algae. *Plant Physiology and Biochemistry* 48: 513-520.

Fuse T, Sasaki T, Yano M. (2001) Ti-plasmid vectors useful for functional analysis of rice genes. *Plant Biotechnology* 18:219-222.

Grienenberger E, Besseau S, Geoffroy P, Debayle D, Heintz D, *et al*. (2009) A BAHD acyltransferase is expressed in the tapetum of *Arabidopsis* anthers and is involved in the synthesis of hydroxycinnamoyl spermidine. *The Plant Journal* 58:246-259.

Groppa MD, Benavides MP. (2007) Polyamines and abiotic stress: recent advances. *Amino Acids* 34:35-45.

Hamana K, Aizaki T, Arai E, Uchikata K, Ohnishi H. (2004) Distribution of norspermidine as a cellular polyamine within micro green algae including non-photosynthetic achlorophyllous Polytoma, Polytomella, Prototheca and Hellicosporidium. *The Journal of General and Applied Microbiology* 50:289-295.

Hamana K, Matsuzaki S. (1985) Distinct difference in the polyamine compositions of Bryophyta and Pteridophyta. *The Journal of Biochemistry* 97:1595-1601.

Handa AK, Mattoo AK. (2010) Differential and functional interactions emphasize the multiple roles of polyamines in plants. *Plant Physiology and Biochemistry* 48: 540-546.

Hood EE, Helmer GL, Fraley RT, Chilton MD. (1986) The hypervirulence of *Agrobacterium tumefaciens* A281 is encoded in a region of pTiBo542 outside of T-DNA. *Journal of Bacteriology* 168:1291-1301.

Kakehi J, Kuwashiro Y, Motose H, Igarashi K, Takahashi T. (2010) Norspermine substitutes for thermospermine in the control of stem elongation in *Arabidopsis thaliana*. *FEBS Letters* 584:3042-3046.

Kakehi J, Kuwashiro Y, Niitsu M, Takahashi T. (2008) Thermospermine is required for stem elongation in *Arabidopsis thaliana*. *Plant Cell Physiology* 49:1342-1349.

Kamada-Nobusada T, Hayashi M, Fukazawa M, Sakakibara H, Nishimura M. (2008) A putative peroxisomal polyamine oxidase, AtPAO4, is involved in polyamine catabolism in *Arabidopsis thaliana. Plant Cell Physiology* 49:1272-1282.

Kim DW, Watanabe K, Murayama C, Izawa S, Niitsu M, Michael AJ, Berberich T, Kusano T. (2014) Polyamine oxidase 5 regulates *Arabidopsis thaliana* growth through a thermospermine oxidase activity. *Plant Physiology* 165:1575-1590.

Kolattukudy PE (1981) Structure, biosynthesis, and biodegradation of cutin and suberin. *Annual Review of Plant Physiology* 32: 539-567.

Knott JM, Römer P, Sumper M. (2007) Putative spermine synthases from *Thalassiosira pseudonana* and *Arabidopsis thaliana* synthesize thermospermine rather than spermine. *The FEBS Letters* 581:3081-3086.

Kuehn GD, Rodriguez-Garay B, Bagga S, Phillips GC. (1990) Novel occurrence of uncdommon polyamines in higher plants. *Plant Physiology* 94:855-857.

Kusano T, Berberich T, Tateda C, Takahashi Y. (2008) Polyamines: essential factors for growth and survival. *Planta* 228:367-381.

Kusano T, Kim DW, Liu T, Berberich T. (2015) Polyamine catabolism in plants. In *Polyamine: A universal molecular nexus for growth, survival and specialized metabolism*, eds. T. Kusano and H. Suzuki (Springer Tokyo), 77-88.

Lim TS, Chitra TR, Han P, Pua EC, Yu H. (2006) Cloning and characterization of *Arabidopsis* and *Brassica juncea* flavin-containing amine oxidases. *Journal of Experimental Botany* 57:4155-4169.

Liu T, Kim DW, Niitsu M, Berberich T, Kusano T. (2014a) *Oryza sativa* polyamine oxidase 1 back-converts tetraamines, spermine and thermospermine, to spermidine. *Plant Cell Reports* 33:143-151.

Liu T, Kim DW, Niitsu M, Maeda S, Watanabe M, Kamio Y, Berberich T, Kusano T. (2014b) Polyamine oxidase 7 is a terminal catabolism-type enzyme in *Oryza sativa* and is specifically expressed in anther organ. *Plant and Cell Physiology* 55:1110-1122.

Liu T, Kim DW, Niitsu M, Berberich T, Kusano T. (2014c) POLYAMINE OXIDASE 1 from rice (*Oryza sativa*) is a functional ortholog of Arabidopsis POLYAMINE OXIDASE 5. *Plant Signaling & Behavior* 9:e29773.

Mattoo AK, Minocha SC, Minocha R, Handa AK. (2010) Polyamines and cellular metabolism in plants: transgenic approaches reveal different responses to diamine putrescine versus higher polyamines spermidine and spermine. *Amino Acids* 38:405-413.

Minguet EG, Vera-Sirera F, Marina A, Carbonell J, Blazquez MA (2008) Evolutinary diversification in polyamine biosynthesis. *Molecular Biology and Evolution* 25:2119-2128.

Moschou PN, Sanmartin M, Andriopoulou AH, Rojo E, Sanchez-Serrano JJ, Roubelakis-Angelakis KA. (2008) Bridging the gap between plant and mammalian polyamine catabolism: a novel peroxisomal polyamine oxidase responsible for a full back- conversion pathway in Arabidopsis. *Plant Physiology* 147:1845-1857.

Moschou PN, Wu J, Cona A, Tavladoraki P, Angelini R, Roubelakis-Angelakis KA. (2012) The polyamines and their catabolic products are significant players in the turnover of nitrogenous molecules in plants. *Journal of Experimental Botany* 63:5003-5015.

Naka Y, Watanabe K, Sagor G.H.M, Niitsu M, Pillai A, Kusano T, Takahashi Y. (2010) Quantitative analysis of plant polyamines including thermospermine during growth and salinity stress. *Plant Physiology and Biochemistry* 48:527-533.

Niitsu M, Samejima K. (1986) Synthesis of a series of linear pentaamines with three and four methylene chain intervals. *Chemical and Pharmaceutical Bulletin* (Tokyo) 34:1032-1038.

Ono Y, Kim DW, Watanabe K, Sasaki A, Niitsu M, Berberich T, Kusano T, Takahashi Y. (2012) Constitutively and highly expressed *Oryza sativa* polyamine oxidases localize in peroxisomes and catalyze polyamine back conversion. *Amino Acids* 42:867-876.

Radova A, Sebela M, Galuszka P, Frebort I, Jacobsen S, *et al*. (2001) Barley polyamine oxidase: characterization and analysis of the co-factor and the N-terminal amino acid sequence. *Phytochemical Analysis* 12:166-173.

Rodriguez-Garay B, Phillips GC, Kuehn GD. (1988) Detection of norspermidine and norspermine in *Medicago sativa* L. (alfalfa). *Plant Physiology* 89:525-529.

Samejima K, Takeda M, Kawase M, Okada M, Kyogoku Y. (1984) Syntheses of ^{15}N-enriched polyamines. *Chemical Pharmaceutical Bulletin* 32:3428-3435.

Sanders PM, Lee PY, Biesgen C, Boone JD, Beals TP, Weiler EW, Goldberg RB. (2000) The Arabidopsis *DELAYED DEHISCENCE1* Gene Encodes an Enzyme in the Jasmonic Acid Synthesis Pathway. *The Plant Cell* 12:1041-1061.

Seiler N. (2004) Catabolism of polyamines. *Amino Acids* 26:217-233.

Seto Y, Sado A, Asami K, Hanada A, Umehara M, Akiyama K, Yamaguchi S. (2014) Carlactone is an endogenous biosynthetic precursor for strigolactones. *Proceedings of the National Academy of Sciences of the United States of America* 111:1640-1645.

Song S, Qi T, Huang H, Xie D. (2013) Regulation of stamen development by coordinated actions of jasmonate, auxin, and gibberellin in *Arabidopsis*. *Molecular Plant* 6:1065-1073.

Song S, Qi T, Wasternack C, Xie D. (2014) Jasmonate signaling and crosstalk with gibberellin and ethylene. *Current Opinion in Plant Biology* 21:112-119

Tabor CW, Tabor H. (1984) Polyamines. *Annual Review of Biochemistry* 53:749-790.

Takahashi, T., and Kakehi, J-I. (2010) Polyamines: ubiquitous polycations with unique roles in growth and stress responses. *Annals of Botany* 105:1-6.

Takahashi Y, Cong R, Sagor GHM, Niitsu M, Berberich T, Kusano T. (2010) Characterization of five polyamine oxidase isoforms in *Arabidopsis thaliana*. *Plant Cell Reports* 29:955-965.

Takano A, Kakehi JI, Takahashi T. (2012) Thermospermine is not a minor polyamine in the plant kingdom. *Plant and Cell Physiology* 53:606-616.

Tamura K, Stecher G, Peterson D, Filipski A, Kumar S. (2013) MEGA6: Molecular evolutionary genetics analysis version 6.0. *Molecular Biology and Evolution* 30:2725-2729.

Tassoni A, Van Buuren M, Franceschetti M, Fornale IS, Bagni N. (2000) Polyamine content and metabolism in Arabidopsis thaliana and effect of spermidine on plant development. *Plant Physiology and Biochemistry* 38:383-393.

Tavladoraki P, Rossi MN, Saccuti G, Perez-Amador MA, Polticelli F, *et al*. (2006) Heterologous expression and biochemical characterization of a polyamine oxidase from Arabidopsis involved in polyamine back conversion. *Plant Physiology* 141:1519-1532.

Tavladoraki P, Shinina ME, Cecconi F, Di Agostino S, Manera F, *et al*. (1998) Maize polyamine oxidase: primary structure from protein and cDNA sequencing. *The FEBS Letters* 426:62-66.

Tiburcio AF, Altabella T, Bitrian M, Alcazar R. (2014) The roles of polyamines during the lifespan of plants: from development to stress. *Planta* 240:1-18.

Toki S, Hara N, Ono K, Onodera H, Tagiri A, Oka S, Tanaka H. (2006) Early infection of scutellum tissue with Agrobacterium allows high-speed transformation of rice. *The Plant Journal.* 47:969-976.

Turner JG, Ellis C, Devoto A. (2002) The Jasmonate Signal Pathway. *The Plant Cell* 14:S153-S164.

Vujcic S, Diegelman P, Bacchi CJ, Kramer DL, Porter CW. (2002) Identification and characterization of a novel flavin-containing spermine oxidase of mammalian cell origin. *Biochemical Journal* 367:665-675.

Vujcic S, Liang P, Diegelman P, Kramer DL, Porter CW. (2003) Genomic identification and biochemical characterization of the mammalian polyamine oxidase involved in polyamine back-conversion. *Biochemical Journal* 370:19-28.

Wallace HM, Fraser AV, Hughes A. (2003) A perspective of polyamine metabolism. *Biochemical Journal* 376:1-14.

Walters DR. (2003) Polyamines and plant disease. *Phytochemistry* 64:97-107.

Wang Y, Devereux W, Woster PM, Stewart TM, Hacker A, Casero RA Jr. (2001) Cloning and characterization of a human polyamine oxidase that is inducible by polyamine analogue exposure. *Cancer Research* 61:5370-5373.

Wasternack C, Stenzel I, Hause B, Hause G, Kutter C, Maucher H, Neumerkel J, Feussner I, Miersch O. (2006) The wound response in tomato - role of jasmonic acid. *Journal of Plant Physiology* 163:297-306.

Weng J-K, Chapple C. (2010) The origin and evolution of lignin biosynthesis. *New Phytologist* 187: 273-285.

Wilson ZA, Zhang D-B. (2009) From Arabidopsis to rice: pathways in pollen development. *Journal of Experimental Botany* 60:1479-1492.

Wu T, Yankovskaya V, McIntire WS. (2003) Cloning, sequencing, and heterologous expression of the murine peroxisomal flavoprotein, N^1-acetylated polyamine oxidase. *Journal of biological chemistry* 278:20514-20525.

Yang F, Zhang Y, Huang Q, Yin G, Pennerman KK, Yu J, Liu Z, Li D, Guo A. (2015) Analysis of key genes of jasmonic acid mediated signal pathway for defense against insect damages by comparative transcriptome sequencing. *Scientific Reports* 5:1650.

Yobi A, Wone BWM, Xu W, Alexander DC, Guo L, Ryals JA, Oliver MJ, Cushman JC (2012) Comparative metabolic profiling between desiccation-sensitive and

desiccation-tolerant species of Selaginella reveals insights into the resurrection trait. *The Plant Journal* 72:983-999.

Yoda Y, Fujimura K, Takahashi H, Munemura I, Uchimiya H, Sano H. (2009) Polyamines as a common source of hydrogen peroxide in host- and nonhost hypersensitive response during pathogen infection. *Plant Molecular Biology* 70:103-112.

Zhu XJ, Thalor SK, Takahashi Y, Berberich T, Kusano T. (2012) An inhibitory effect of the sequence-conserved upstream open reading frame on the translation of the main open-reading frame of *HsfB1* transcripts in Arabidopsis. *Plant Cell and Environment* 35:2014-2030.

Publication list

G.H.M. Sagor[†], Masataka Inoue[†], Dong Wook Kim, Seiji Kojima, Masaru Niitsu, Thomas Berberich, Tomonobu Kusano (2015) The polyamine oxidase from lycophyte *Selaginella lepidophylla* (SelPAO5), unlike that of angiosperms, back-converts thermospermine to norspermidine. FEBS Lett. 589: 3071-3078

([†]The first two authors contributed equally to this work)

Related publication

Kunihiro S, Saito T, Matsuda T, Inoue M, Kuramata M, Taguchi-Shiobara F, Youssefian S, Berberich T, Kusano T (2013) Rice *OsDEP1*, encoding a highly cysteine-rich G protein γ subunit, confers cadmium-tolerance to yeast cells and plants. J Exp Botany 64: 4517-4527.

Acknowledgements

I thank Dr. Yoshiya Seto (Tohoku University) for help with the LC-MS/MS analysis. Mr. Kiyoshi Ishikawa is acknowledged for his guidance in cultivating *Selaginella* plants. I also thank Dr. Thomas Berberich (Biodiversity and Climate Research Center) for critical reading of my Ph. D. thesis.